Changes in Histotone Isoform Abundnance and Histone Post-Translational Modifications during Anoxia Tolerance and Recovery in WS40NE cells of *Austrofundulus limnaeus*

Chelsea Hughes[1], Elizabeth A. Mojica[2], Dietmar Kültz[2], Jason E. Podrabsky[1]

1. Department of Biology, Center for Life in Extreme Environments, Portland State University, P.O. Box 751, Portland, OR 97201, USA

2. Department of Animal Sciences and Genome Center, University of California, Davis, One Shields Avenue, Meyer Hall, Davis, CA 95616, USA

Keywords: mass spectrometry; epigenetics; histone post-translational modifications; anoxia; stress tolerance

Abstract

Anoxia is an often-lethal stressor to vertebrates, yet some vertebrates have adapted cellular mechanisms to survive in anoxic conditions. Embryos of the annual killifish *Austrofundulus limnaeus* have the greatest tolerance to anoxia of all vertebrates, yet the epigenetic mechanisms that support their anoxia tolerance are unknown. Using mass spectrometry, 1043 unique biologically relevant histone post-translational modifications (unimod+histone residue) were detected in WS40NE cells, representing thirteen types of biologically relevant histone post-translational modifications (hPTMs) present during normoxia, 1 d anoxia, 4 d anoxia, and aerobic recovery from anoxia. Of these 1043 hPTMs, 816 were significantly differentially expressed in at least one comparison. Thirty-six significant hPTMs were considered highly condition dependent. Additionally, at least four histone isoforms were differentially expressed, representing H2A, H2B, and H3 isoforms. Our data suggests that specific histone modifications as well as changes in histone isoform abundance in WS40NE cells may be necessary to successfully respond to extreme changes in oxygen availability.

Introduction

All organisms must respond to their environment, which offers both opportunities and threats. By changing which genes are expressed, organisms can modify their phenotype to take advantage of opportunities and neutralize threats. However, environmental stressors can often lead to aberrant gene expression in organisms that lack these adaptations. This is particularly true during anoxic stress in mammals, which can cause apoptosis and inappropriate reentry into the cell cycle in mammalian cells [1, 2]. Specifically in mammalian neurons, apoptosis is associated with cellular dysregulation that leads these terminally differentiated cells to re-enter the cell

35 cycle, which often leads to catastrophic cell failure [2]. Additionally, mitochondrial
36 dysregulation is associated with anoxia due to inhibition of the electron transport chain (ETC)
37 and depolarization of the inner mitochondrial membrane that can lead to apoptosis [3-5]. The
38 subsequent cell death causes tissue damage, which continues when oxygen is returned to the
39 affected area, a phenomenon known as ischemia-reperfusion injury in mammals [6]. Ischemia-
40 reperfusion increases reactive oxygen species (ROS) such as the superoxide anion (O^{-2}),
41 hydrogen peroxide (H_2O_2), and hydroxyl radical (OH^-) [7]. While low levels of ROS are a
42 normal byproduct of mitochondrial metabolism [8], high levels of ROS can lead to neuronal
43 death within 5 minutes [9, 10]. In contrast, a handful of vertebrates have adapted mechanisms to
44 modify their gene expression to survive environmental stressors, including osmotic, thermal,
45 ROS, and anoxia with little or no damage [11-19].Therefore, there is a need to understand how
46 gene expression is regulated in anoxia tolerant vertebrates to understand how they avoid these
47 fates. This study focuses on epigenetic histone modifications in response to anoxia in a cell line
48 isolated from anoxia-tolerant embryos of the annual killifish, *Austrofundulus limnaeus*.

49 Epigenetic responses to a variety of stressors are documented in multiple organisms [20-23].
50 However, few histone post-translational modifications (hPTMs) have been investigated in
51 response to hypoxia or anoxia. Additionally, these data often come from anoxia intolerant
52 organisms that are experiencing a disease state and are likely failing [24, 25]. Additionally, this
53 research often focuses only on well-known residues and specific types of hPTMs such as
54 methylation [26, 27]. For example, histone-3 lysine-4 trimethylation (H3K4me3) and
55 H3K36me3 are known to change in HeLa cells within 1 h of hypoxic exposure, but HeLa cells
56 begin to die within 1 d of severe hypoxia [28, 29]. Limited research exists on histone
57 modifications in anoxia tolerant organisms, but this work again focuses on well-known

58 modifications such as acetylation and methylation [30]. It is unknown how less studied hPTMs,
59 such as lactylation, 4-hydroxynonenal, and oxidation are impacted by anoxic stress, particularly
60 in anoxia tolerant species. Even better characterized hPTMs like ubiquitylation are not well
61 understood in anoxia. While ubiquitylation of the proteome has been studied in ischemia and
62 anoxia recovery [31, 32], to our knowledge, anoxia-induced histone ubiquitylation has never
63 been explored in a continuous cell line.

64 Embryos of the annual killifish *Austrofundulus limnaeus* have the greatest tolerance to anoxia of
65 all vertebrates, making them the ideal model to study the cellular mechanisms necessary for
66 anoxia tolerance. This remarkable tolerance of anoxia is supported by the ability of embryos to
67 arrest development and enter a state of anoxia-induced quiescence [33]. The global histone
68 landscape of developing embryos (Wourms' Stage 36) under normoxia and after 24 h of anoxia
69 suggests a stabilization of both histone isoform and hPTM abundance [34]. This is surprising, as
70 hPTMs are known to respond to stressors quickly [22, 28, 35, 36]. However, this stabilization
71 represents an averaged histone landscape for multiple cell types [34]. It is unclear how specific
72 cell lines of *A. limnaeus* respond to anoxia, particularly in the absence of tissue-dependent cell
73 signaling. Additionally, no research has investigated how the histone landscape of *A. limnaeus*
74 changes when exposed to longer bouts of anoxia or during recovery from anoxia.

75 PSU-AL-WS40NE (from now on WS40NE) is a neuroepithelial cell line that was isolated from
76 an embryonic (Wourms' Stage 40) *A. limnaeus* tissue explant. These cells can survive for at least
77 49 days without oxygen [37], while SH-SY5Y human neuroblastoma cells can survive anoxia for
78 only approximately 1.3 days [38], and mouse N2A cells can survive for just over 3 days [37].
79 Here, we describe for the first time the global histone landscape of WS40NE cells exposed to

80 anoxia and recovery from anoxia. We hypothesize cells undergo extensive changes to histone
81 isoforms and the hPTM landscape in response to anoxia and aerobic recovery from anoxia.

82 **Results**

83 ***Histone Abundance***

84 Our methods resulted in the identification of 1,927 peptides across at least twenty-three distinct
85 histone proteins based on their unique protein accession number. These proteins were
86 representative of H1, H2A, H2B, and H3 isoforms. No H4 isoforms were detected. Sequence
87 coverage ranged from 17-100% (Fig. 1). At least four histones were differentially expressed
88 across the four experimental time points (Fig. 1).

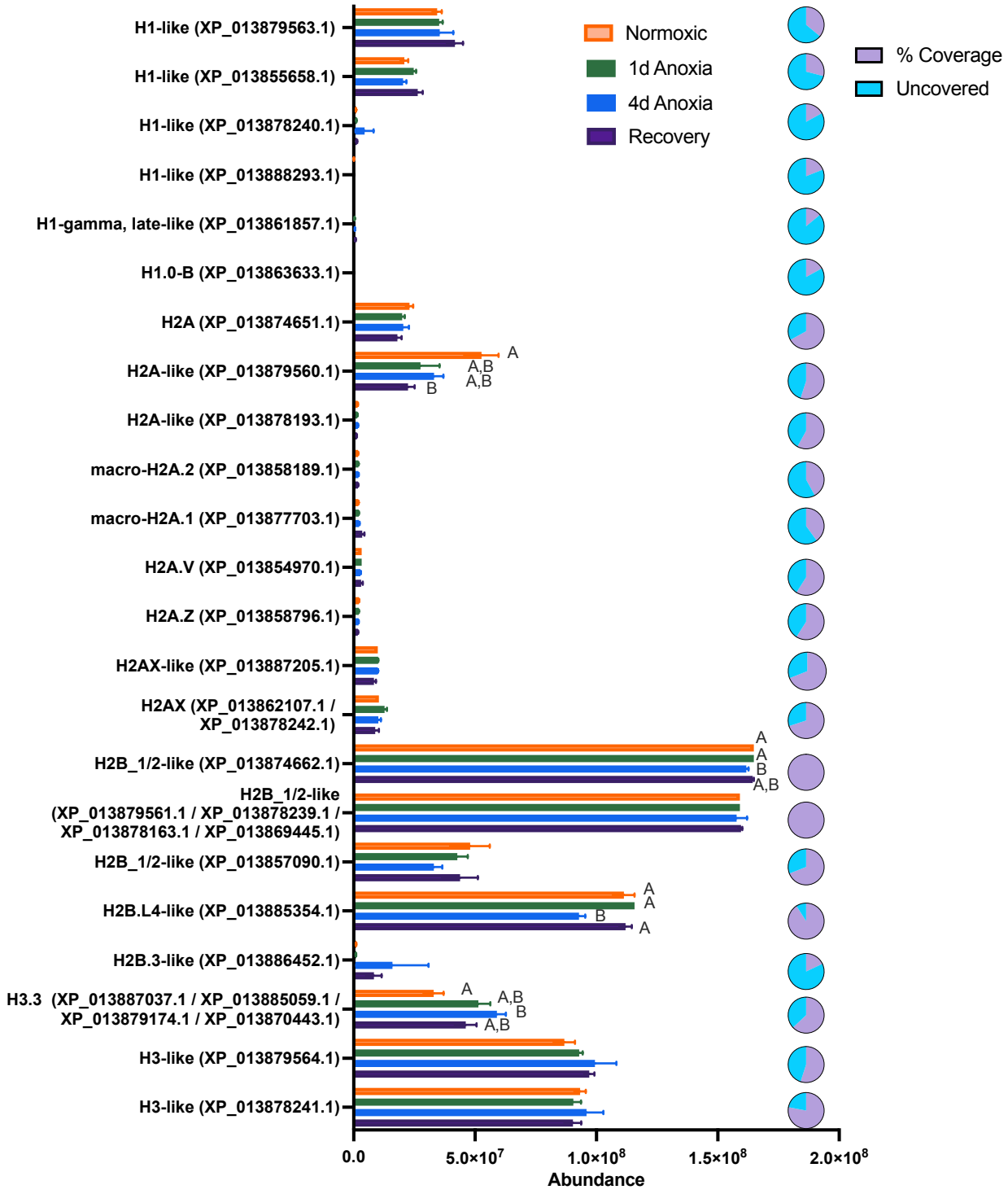

89

90 **Figure 1. Histone isoform abundance in WS40NE cells.** Twenty distinct histone proteins were identified based on

91 their unique protein accession number, as well as three groups of histones that could not be distinguished. Bar

92 graphs represent the quantile normalized mean ± SEM of histone relative abundance during normoxia (orange), 1 d
93 anoxia (green), 4 d anoxia (blue), and 1 d of recovery (dark purple). Letters over bars represent statistically
94 significant isoform abundances determined by pairwise comparisons. Pie charts represent the sequence coverage
95 (light purple) and the percent of peptide sequences that were not detected (blue) for each isoform. Sequence
96 coverage is defined as the total observed protein sequence length divided by the total protein length. Note that due to
97 different peptide ionization efficiencies, histone isoform abundance can only be compared across conditions and not
98 to one another within a condition.

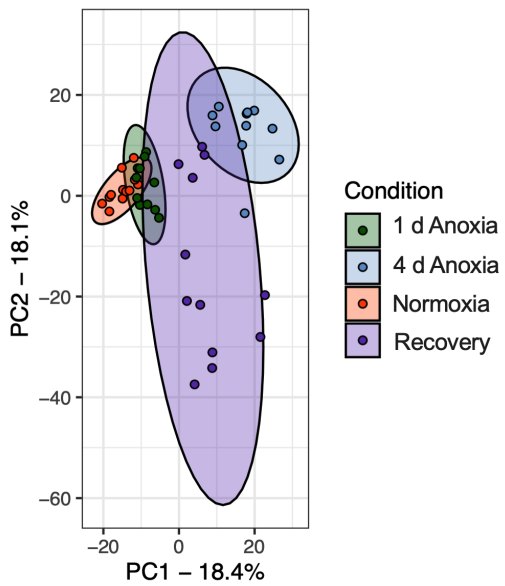

A histone H3.3 protein increased significantly within 1 d of anoxia, while an H2A-like protein decreased across this same time frame. Two histone H2B isoforms decreased in abundance after 4 d of anoxia. However, principal component analysis demonstrated broad sample similarity across conditions when considering the abundances of all histone isoforms (Fig. 2).

107 **Figure 2. Principal component analysis of histone isoform abundance in WS40NE cells exposed to anoxia and**
108 **aerobic recovery from anoxia.** The mean quantile normalized abundance values of all histone isoforms were used
109 to construct a PCA Plot. Normoxic (purple), 1 d anoxic (green), 4 d anoxic (blue), and recovery samples (pale blue)
110 are plotted according to PC1 and PC2 with a 95% confidence ellipse surrounding each cluster.

111 ***Histone Post-translational Modifications***

112 Histone groups were evaluated in a residue-specific manner to determine specific sites of
113 differential modification. Principal component analysis (PCA) illustrates that, globally, the
114 hPTM landscape is most unique after 4 d of anoxia compared to normoxia (Fig. 3A). It is worth
115 noting the high variation in PC2 for the recovery time point (Fig. 3A). Out of 1293 unique

116 hPTMs detected, 1043 unique hPTMs (hPTM type+residue) were considered biologically
117 relevant, representing thirteen types of biologically relevant PTMs (Fig. 3B,C). Four hundred
118 and sixty-one residues were modified with biologically relevant hPTMs, with many residues
119 being modified with multiple types of hPTMs. These types of modifications included commonly
120 studied modifications such as acetylation, methylation, phosphorylation, and ubiquitylation, and
121 less studied modifications such as lactylation and 4-hydroxynonenal. All thirteen types of
122 modifications were statistically significant on at least one residue in at least one comparison,
123 with oxidation/hydroxylation and dioxidation having the greatest number of significantly
124 modified residues, followed closely by dehydration and phosphorylation (Fig. 3B). As expected,
125 the percent sequence coverage is positively correlated with the number of significant hPTMs
126 (Fig. 3D, $r = 0.7$, $p = 0.0003$), and thus for certain histones our ability to draw global conclusions
127 is somewhat limited. Of the unique biologically relevant PTMs detected, 816 were significant in
128 at least one comparison (Fig. 3E). Hundreds of significant differential hPTMs were present
129 across all four timepoints with 4 d of anoxia having the highest number compared to other time
130 points (Fig. 3E).

131

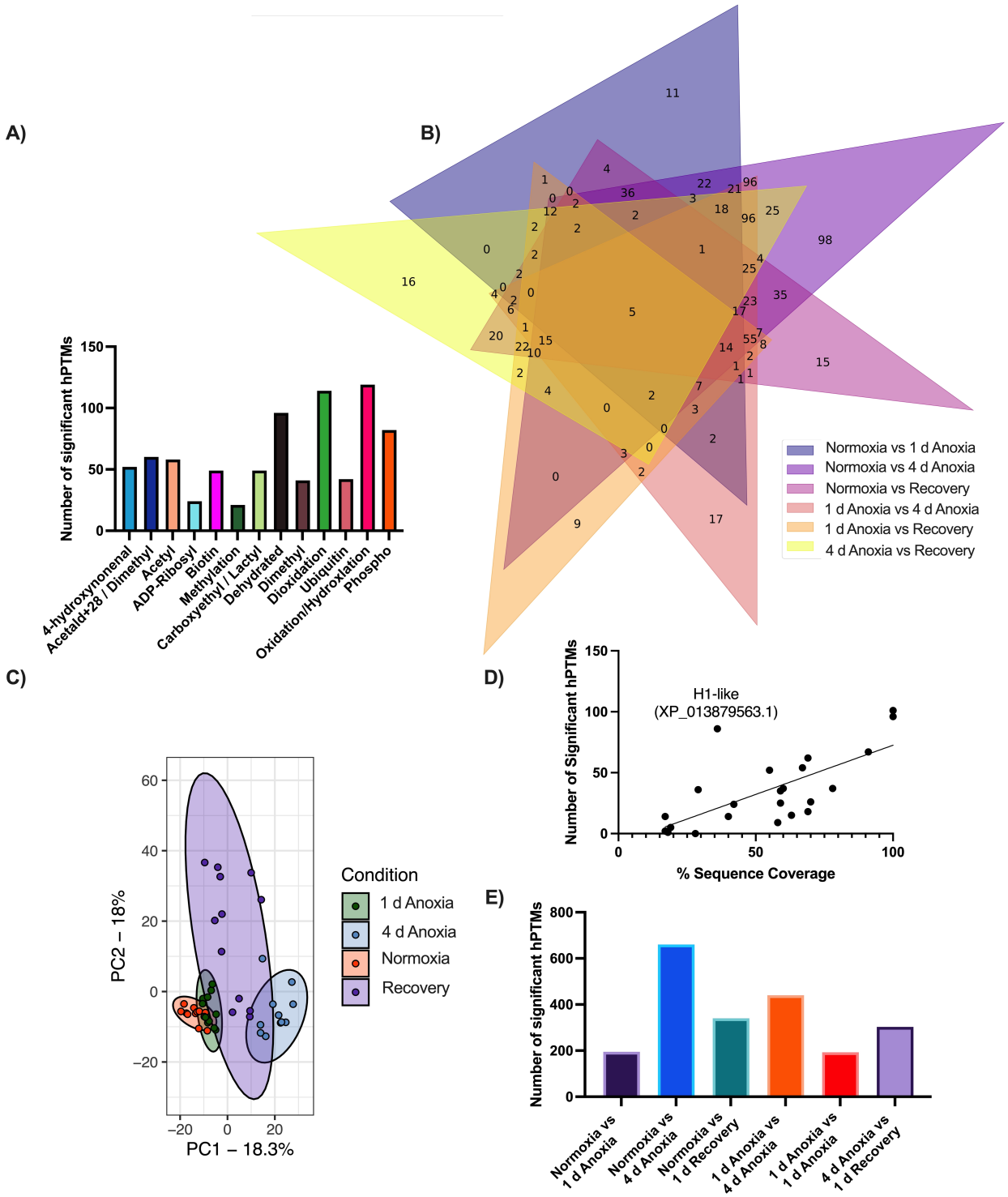

Figure 3. Quantification of global patterns of significant histone post-translational modifications in WS40NE cells exposed to anoxia and recovery from anoxia. (A) The number of significant hPTMs across all histone

135 isoforms plotted by modification type**. (B)** Venn diagram illustrating the occurrence of the 297 unique and
136 biologically-relevant hPTMs across the experimental conditions used in this study. **(C)** PCA plot of the M-values of
137 all hPTMs indicate that hPTM patterns at 4 d of anoxia are unique compared to the other experimental conditions. It
138 is also noteworthy that variation in global patterns of hPTMs appears to be high during aerobic recovery. Individual
139 samples (data points) are surrounded by 95% confidence ellipses for each treatment group. **(D)** There is a positive
140 correlation ($r = 0.7$, $p = 0.0003$) between percent sequence coverage for each histone isoform and the number of
141 significant hPTMs identified. However, several isoforms do not follow this trend, suggesting these are highly
142 modified isoforms. **(E)** The bar graph represents the number of significantly expressed hPTMs in each t-test
143 comparison.

144 Thirty hPTMs were highly abundant (having an average relative abundance of 50% or greater)
145 across all conditions. Of the high abundance hPTMs, 15 displayed an average relative abundance
146 across all samples of exactly 100% during all conditions, meaning that each specific residue was
147 always modified by that PTM (Table 1). Five histones had at least one hPTM site with 100%
148 relative abundance, representing H1, H2A, and H3 histones. At least 8 distinct types of PTMs are
149 represented in this group with dehydration accounting for 30% of these stable modifications.

150

151 **Table 1. Histone post-translational modifications with 100% relative abundance in WS40NE cells.** Fifteen
152 hPTMs, across 5 histone isoforms, always had the same hPTM across all experimental conditions. At least eight
153 distinct types of PTMs are represented.
154

155

Protein Accession	Protein Description	Amino Acid + Position	PTM Description
XP_013861857.1	H1-gamma,_late-like	196K	Acetylation
XP_013861857.1	H1-gamma,_late-like	175K	Biotinylation
XP_013861857.1	H1-gamma,_late-like	173P	Oxidation/Hydroxylation
XP_013861857.1	H1-gamma,_late-like	191K	Acetylation
XP_013861857.1	H1-gamma,_late-like	157K	Acetylation
XP_013861857.1	H1-gamma,_late-like	228K	Dioxidation
XP_013861857.1	H1-gamma,_late-like	24R	4-hydroxynonenal
XP_013861857.1	H1-gamma,_late-like	46S	Phosphorylation
XP_013878240.1	H1-like	64S	Dehydrated
XP_013885354.1	H2B.L4-like	46S	Dehydrated
XP_013885354.1	H2B.L4-like	55S	Dehydrated
XP_013885354.1	H2B.L4-like	43T	Dehydrated
XP_013885354.1	H2B.L4-like	31Y	Dehydrated
XP_013878241.1	H3-like	24R	Oxidation/Hydroxylation
XP_013878241.1	H3-like	17K	Oxidation/Hydroxylation

156 Individual hPTMs at specific residues were also evaluated, and the most condition-dependent
157 hPTMs were identified. Significant differential modifications were detected on all groups of
158 histones (H1, H2A, H2B, H3), with H1-gamma late-like (XP_013861857.1) being the only
159 isoform that did not have any significant hPTMs detected. Thirty-seven hPTMs were considered
160 highly condition dependent, being significantly differentially expressed across 5-6 comparisons
161 (Table 2).
162
163 **Table 2. Highly condition-dependent histone post-translational modifications in WS40NE cells exposed to**
164 **anoxia and aerobic recovery from anoxia.** To be considered highly condition-dependent, hPTMs had to be
165 significant across at least 5 of 6 different comparisons. Thirty-seven hPTMs were selected as the most condition
166 dependent. Differential modifications of histone residues were evaluated using a two-tailed t-test with the
167 Benjamini-Hochberg correction applied to account for multiple hypothesis testing.
168

Protein Accession	Protein Description	Amino Acid + Position	PTM Description
XP_013863633.1	H1.0-B	25K	Acetylation
XP_013863633.1	H1.0-B	19K	4-hydroxynonenal
XP_013879563.1	H1-like	17K	Acetylation
XP_013879563.1	H1-like	51K	4-hydroxynonenal
XP_013879563.1	H1-like	63S	Phosphorylation
XP_013879563.1	H1-like	62R	Oxidation/Hydroxyl
XP_013878193.1	H2A-like	102S	Dehydration
XP_013879560.1	H2A-like	123K	Carboxyethyl/ lactylation
XP_013854970.1	H2A.V	116K	Oxidation/hydroxylation
XP_013854970.1	H2A.V	121K	Biotinylation

XP_013854970.1	H2A.V	122K	Dioxidation
XP_013885354.1	H2B.L4-like	74Y	Phosphorylation
XP_013885354.1	H2B.L4-like	78S	Ubiquitylation
XP_013885354.1	H2B.L4-like	79T	Dehydration
XP_013885354.1	H2B.L4-like	79T	Phosphorylation
XP_013885354.1	H2B.L4-like	82S	Dehydration
XP_013885354.1	H2B.L4-like	83R	Oxidation/hydroxylation
XP_013885354.1	H2B.L4-like	116K	Methylation
XP_013879561.1 /			
XP_013878239.1 /			
XP_013878163.1 /			
XP_013869445.1	H2B_1/2	41Y	Phosphorylation
XP_013879561.1 /			
XP_013878239.1 /			
XP_013878163.1 /			
XP_013869445.1	H2B_1/2	84K	4-hydroxynonenal
XP_013879561.1 /			
XP_013878239.1 /			
XP_013878163.1 /			
XP_013869445.1	H2B_1/2	89T	Phosphorylation
XP_013879561.1 /			
XP_013878239.1 /			
XP_013878163.1 /			
XP_013869445.1	H2B_1/2	90S	Dehydration
XP_013879561.1 /			
XP_013878239.1 /			
XP_013878163.1 /			
XP_013869445.1	H2B_1/2	90S	Phosphorylation

XP_013879561.1 /			
XP_013878239.1 /			
XP_013878163.1 /			
XP_013869445.1	H2B_1/2	114T	Dehydration
XP_013879561.1 /			
XP_013878239.1 /			
XP_013878163.1 /			
XP_013869445.1	H2B_1/2	124K	Methylation
XP_013857090.1	H2B_1/2-like	41Y	Phosphorylation
XP_013857090.1	H2B_1/2-like	78R	Dioxidation
XP_013857090.1	H2B_1/2-like	81H	4-hydroxynonenal
XP_013857090.1	H2B_1/2-like	84K	Acetald+28 / Dimethylation
XP_013874662.1	H2B_1/2	35S	Phosphorylation
XP_013874662.1	H2B_1/2	41Y	Phosphorylation
XP_013874662.1	H2B_1/2	55S	Phosphorylation
XP_013874662.1	H2B_1/2	63S	Ubiquitylation
XP_013874662.1	H2B_1/2	86S	Phosphorylation
XP_013874662.1	H2B_1/2	89T	Phosphorylation
XP_013874662.1	H2B_1/2	90S	Phosphorylation
XP_013874662.1	H2B_1/2	124K	Methylation

Globally, hPTMs did not cover the majority of the residues that are theoretically available. Lysine residues were the most modified with 48.7-51.4% of the available residues modified across the different experimental conditions (Fig. 4A). The modification of specific amino acid residues varied based on experimental conditions (Fig. 4A). Lysines had the most types of modifications, with 10 distinct hPTMs detected globally, and of these, oxidation/hydroxylation, dioxidation, and acetylation were the most common (Fig. 4A). Serine (S) had the second most

176 types of modifications, with 5 distinct hPTMs occurring globally; dehydration and
177 phosphorylation dominated serine modifications (Fig. 4A). Globally, there were significant
178 changes in all types of hPTMs across all six comparisons (Fig. 4B,C): (a) 5 comparing normoxia
179 to 24 h anoxia, (b) 12 comparing normoxia to 4 d anoxia, (c) 8 comparing normoxia to 24 h
180 recovery,(d) 6 comparing 24 h anoxia to 4 d anoxia, (e) 4 comparing 24 h anoxia to 24 h
181 recovery, and (f) 2 comparing 4 d anoxia to 24 h recovery. The majority of the most common
182 modifications decreased significantly during anoxia and remained low even after 24 h of aerobic
183 recovery (Fig. 4B,C). Notably, acetylation, dehydration, oxidation, and dioxidation all increase
184 during anoxia. (Fig. 4B,C).
185

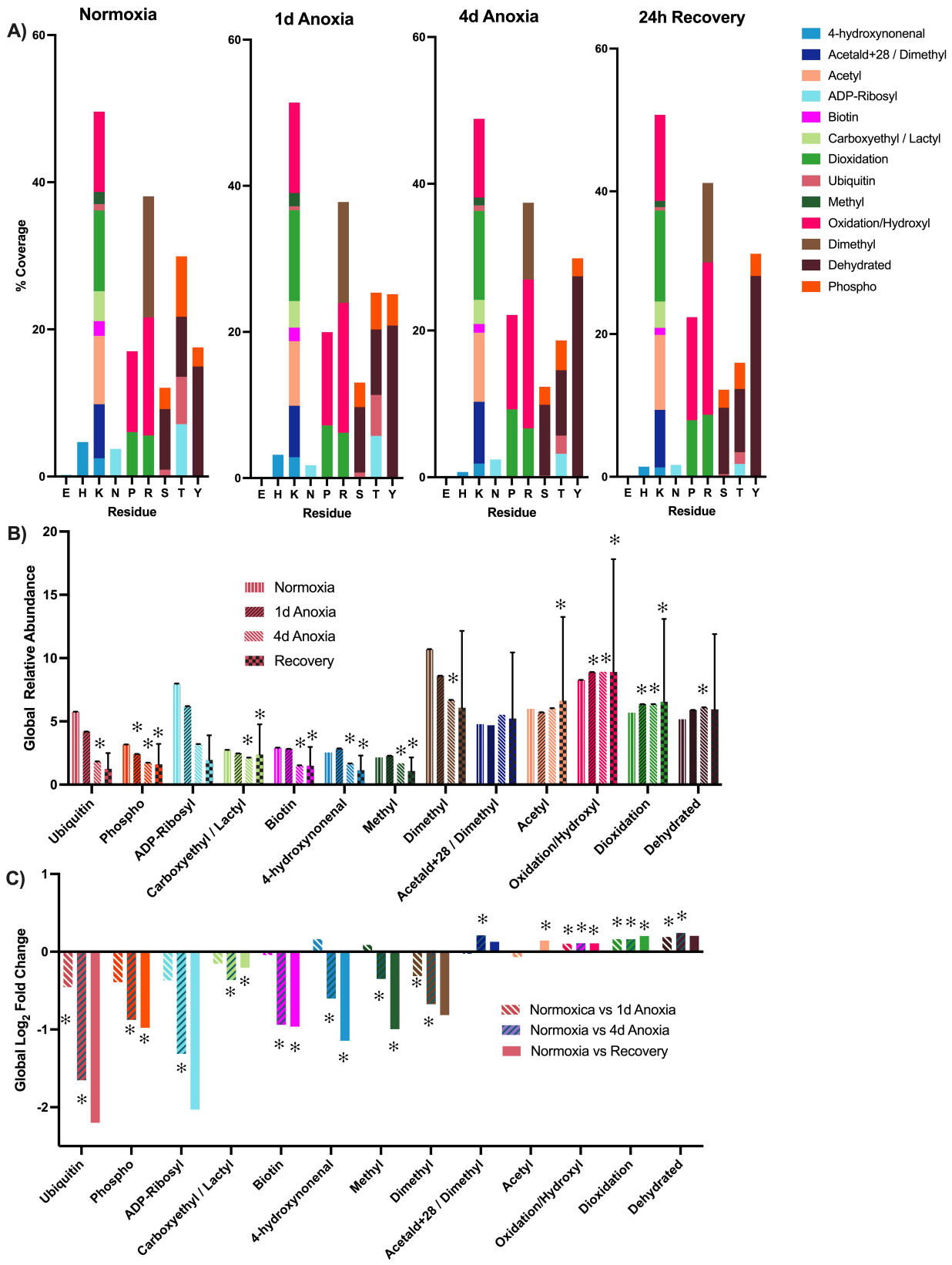
A)
Normoxia
1d Anoxia
4d Anoxia
24h Recovery
% Coverage
Residue
E H K N P R S T Y
4-hydroxynonenal
Acetald+28 / Dimethyl
Acetyl
ADP-Ribosyl
Biotin
Carboxyethyl / Lactyl
Dioxidation
Ubiquitin
Methyl
Oxidation/Hydroxyl
Dimethyl
Dehydrated
Phospho
B)
Global Relative Abundance
Normoxia
1d Anoxia
4d Anoxia
Recovery
Ubiquitin
Phospho
ADP-Ribosyl
Carboxyethyl / Lactyl
Biotin
4-hydroxynonenal
Methyl
Dimethyl
Acetald+28 / Dimethyl
Acetyl
Oxidation/Hydroxyl
Dioxidation
Dehydrated
C)
Global Log2 Fold Change
Normoxica vs 1d Anoxia
Normoxia vs 4d Anoxia
Normoxia vs Recovery

186

187 **Figure 4. Global changes in the histone PTM landscape of WS40NE cells during anoxia and aerobic recovery**
188 **from anoxia. (A)** Thirteen types of hPTMs were detected across nine types of amino acid residues in WS40NE
189 cells. While most residue types are unmodified, lysine (K) residues were the most consistently modified (54.7 -
190 58.3%) across the different experimental conditions. **(B)** From a global perspective, the abundance of most hPTMs
191 decreases in response to anoxia and fails to return to normoxic values after 1 d of aerobic recovery. Acetylation,
192 oxidation, dioxidation and dehydration increase modestly in response to anoxia. Fold change data were calculated
193 from the global mean abundance data for each hPTM.
194

195 ***Characterization of histone H1***

196 Six H1 proteins were identified: (**A**) H1-like (XP_013879563.1), (**B**) H1-like
197 (XP_013855658.1), (**C**) H1-like (XP_013878240.1), (**D**) H1-like (XP_013888293.1), (**E**) H1-
198 gamma late-like (XP_013861857.1), and (**F**) H1.0-B (XP_013863633.1). Thirteen types of
199 PTMs were identified across these isoforms (Figs. 5A). Interestingly, H1-like (XP_013879563.1)
200 appears to carry more modifications compared to the other isoforms even when percent coverage
201 is taken into account (Figs. 1, 3D, 5C). Nine of the 15 modifications with an average relative
202 abundance of exactly 100% in all samples are H1 isoforms, with H1-gamma late-like
203 (XP_013861857.1) having 8 of the 10 (Table 1).
204

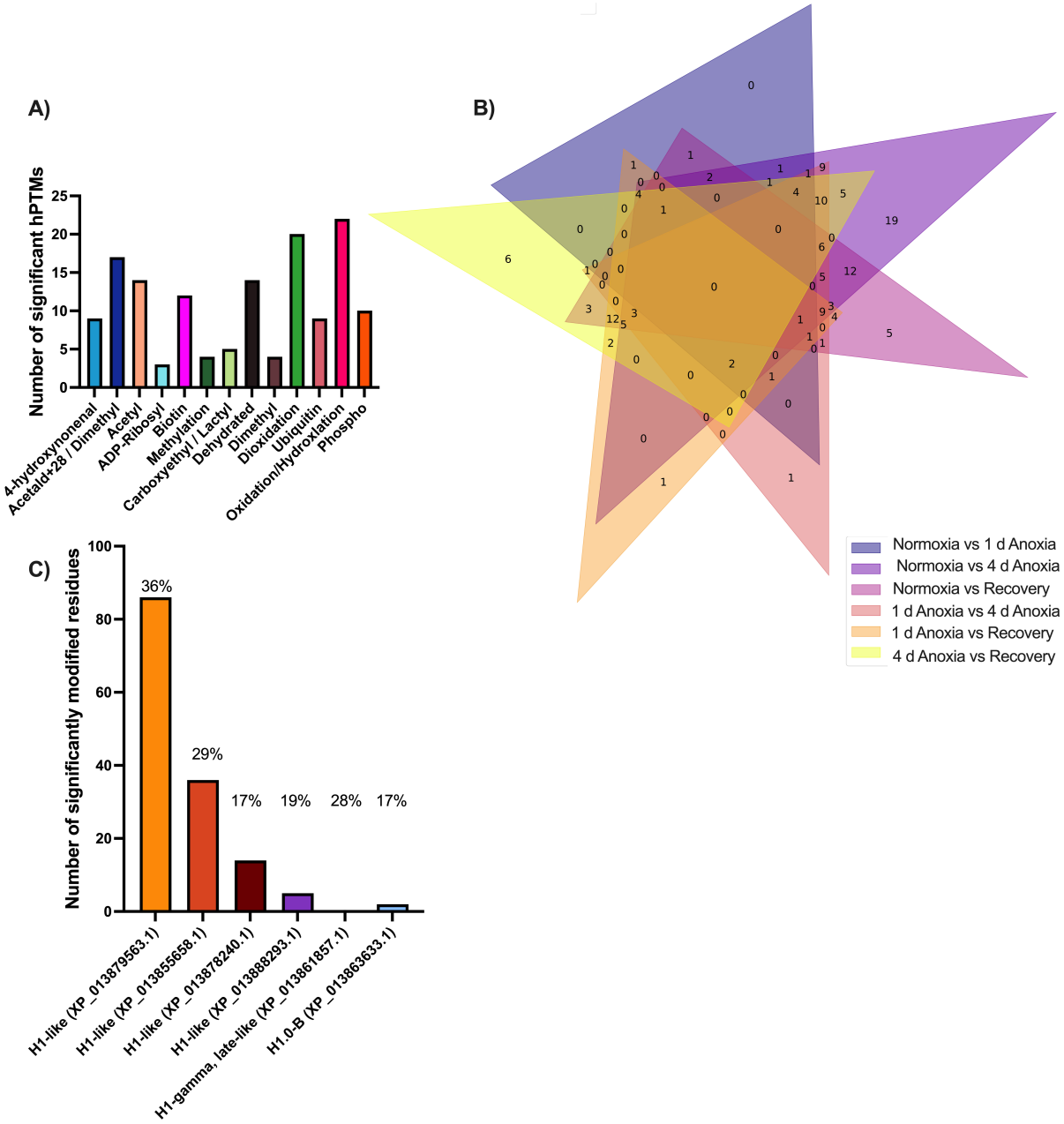

Figure 5. Significant differential histone post-translational modifications on histone H1 isoforms in WS40NE cells. (**A**) The most commonly significant differential hPTM across H1 isoforms were oxidation (22 hPTMs), dioxidation (20 hPTMs), and acetald+28/dimethylation (17 hPTMs). (**B**) Venn diagram illustrating the occurrence of unique and biologically-relevant hPTMs on H1 histone isoforms across experimental treatment groups. (**C**) Five of the six H1 histone isoforms had residues with significantly different hPTM modifications in response to anoxia. The percentage above each bar represents the peptide sequence coverage of that isoform. Note that H1-gamma late-like is modified, but those modifications are stable across experimental treatment groups.

213

214 All six H1 isoforms had residues with significant hPTM modifications, while 5 isoforms had at
215 least one hPTM that changed in relative abundance in response to experimental treatments. One
216 hundred and forty-three significant hPTMs were present on H1 isoforms in at least one condition
217 (Fig. 5). The most common differential modifications in response to the experimental treatments
218 across H1 isoforms were oxidation (22 significant unique hPTMs), dioxidation (20 significant
219 unique hPTMs), and acetald+28/dimethylation (17 significant unique hPTMs) (Fig. 5). Six
220 highly condition-dependent hPTMs were significant across five different comparisons: H1-like
221 (XP_013879563.1) 17K acetylation, 62R oxidation/hydroxylation, and 63S phosphorylation; H1-
222 like (XP_013855658.1) 51K 4-hydroxynonenal; and H1.0-B (XP_013863633.1) 19K 4-
223 hydroxynonenal and 25K acetylation (Fig. 6 and Table 2).

224

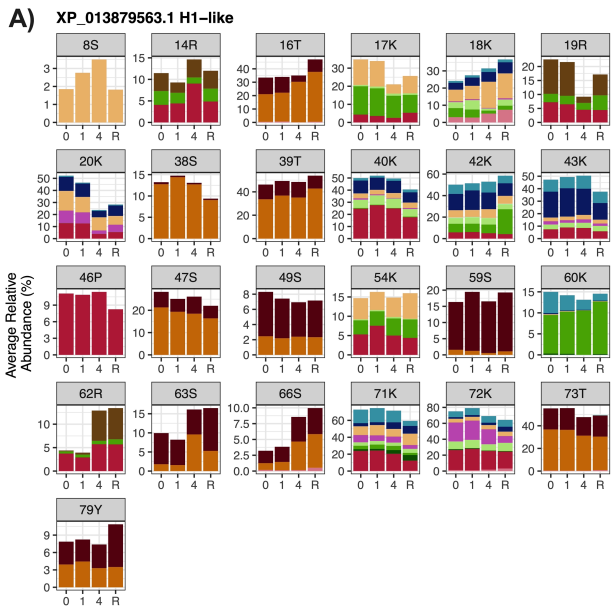

Peptide sequence:
MSELQSDSLSVLQRQTKKRKMAEVAPAPAPAKAAKKKSTKLKK
VGPSVSELIVKAVAASKERSGVSAAALKKTLAAGGYDVDKNKA
RVKTAIKSLVTKGTLVQTKGIGASGSFKMNKQADTKAKKPAAKK
PAPKAKKPAAKKPAAAKKPKKAAAAAKKPAAAKKSPKKAKKPA
AAAKNAAKSPKKTTKSPKKVVKKAPAAKKSPAKKAAKPKAKKA
APKKK

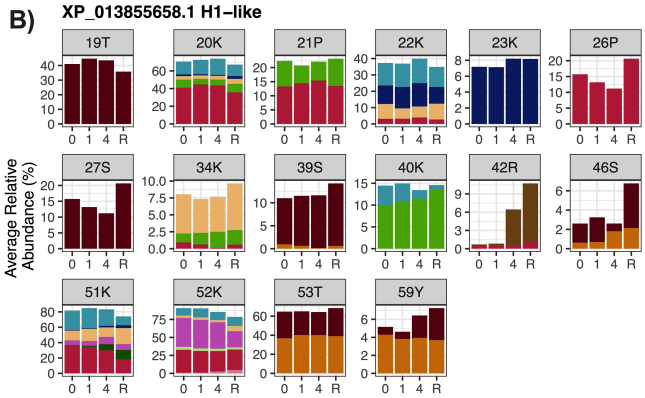

Peptide sequence:
MAEVAPAPAPAKAAKKKSTKPKKAGPSVSELIVKAVAASK
ERSGVSAAALKKTLAAGGYDVDKNKARVKTAIKSLVTKG
TLVQTKGIGASGSFKMNKQADSKAKNPAAKKAAPKAKK
PAAKKPAAAKKPKKPAAAAKKPAAAKKSPKKAKKPAAAA
KKAAKSPKKTTKSPKKVVKKAPAAKKSPAKKAAKPKAKK
AAPKKK

225

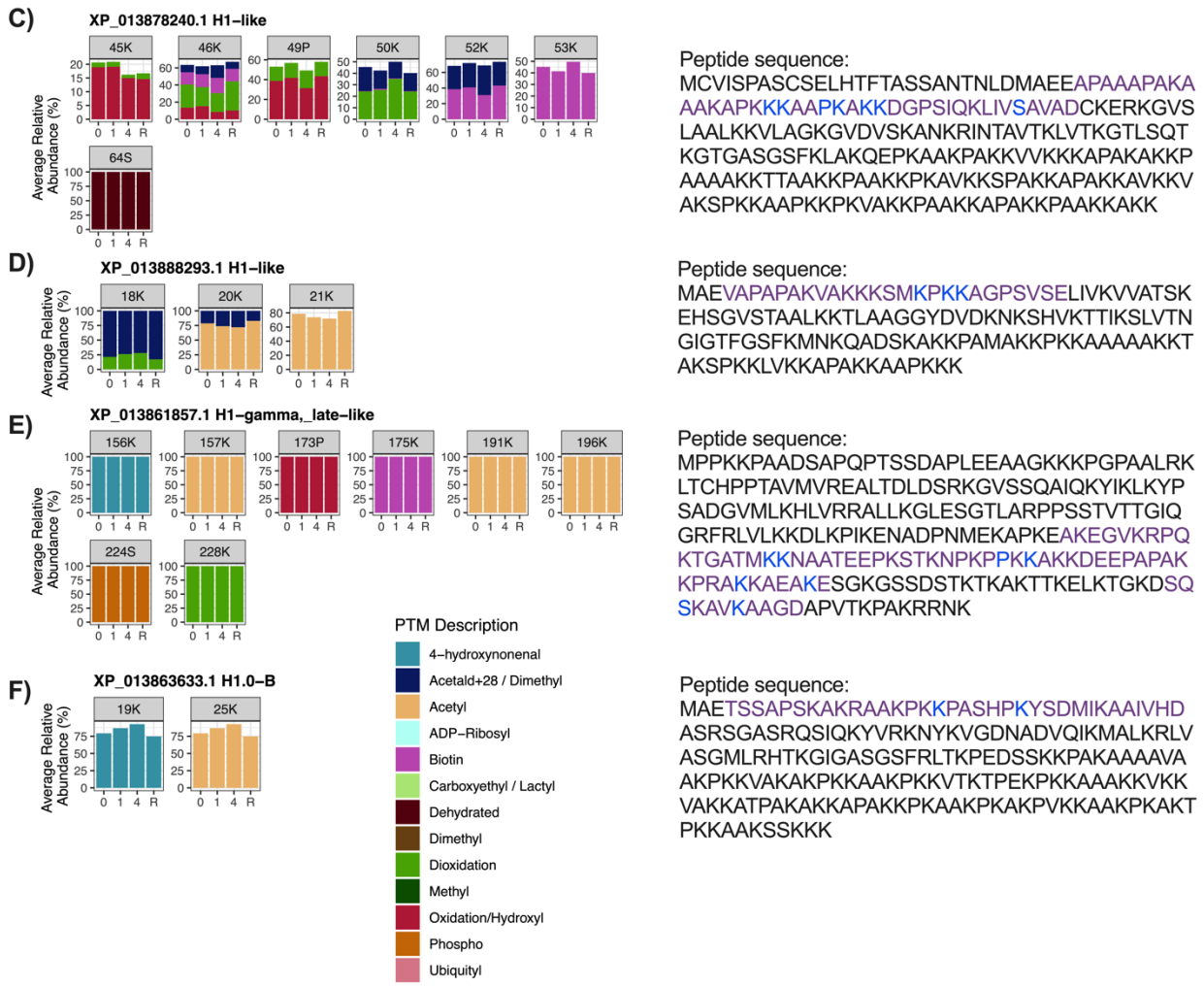

Figure 6. Characterization of post-translational modifications on Histone H1 isoforms in WS40NE cells exposed to anoxia and aerobic recovery from anoxia. Isoforms represented are (**A**) H1-like (XP_013879563.1), (**B**) H1-like (XP_013855658.1), (**C**) H1-like (XP_013878240.1), (**D**) H1-like (XP_013888293.1), (**E**) H1-gamma late-like (XP_013861857.1), and (**F**) H1.0-B (XP_013863633.1). Each panel represents a different amino acid position where at least one hPTM was detected. Amino acid residues are abbreviated using their one letter code. The x-axis displays the condition of the samples: 0 d in anoxia (0), 1 d in anoxia (1), 4 d in anoxia (4), or 1 d of aerobic recovery from 4 d of anoxia (R). The y-axis scales differ across panels to better visualize changes in low abundance hPTMs. Detected (purple) and modified (blue) peptides and the entire peptide sequences for each isoform are listed beside the panels.

Characterization of histone H2A

237 Nine H2A proteins were identified: (**A**) H2A (XP_013874651.1), (**B**) H2A-like
238 (XP_013879560.1), (**C**) H2A-like (XP_013878193.1), (**D**) macro-H2A.2 (XP_013858189.1), (**E**)
239 core histone macro-H2A.1 (XP_013877703.1), (**F**) H2A.V (XP_013854970.1), (**G**) H2A.Z
240 (XP_013858796.1), (**H**) H2AX-like (XP_013887205.1), and (**I**) H2AX-like (XP_013862107.1/
241 XP_013878242.1). Thirteen types of PTMs were identified across these isoforms (Fig. 7A) with
242 257 hPTMs significantly differentially abundant on H2A isoforms in at least one condition (Fig.
243 7B). All nine H2A isoforms had residues with significant hPTM modifications, with H2A
244 (XP_013874651.1) and H2A-like (XP_013879560.1) appearing to have a high proportion of
245 hPTMs for their percent coverage in the data (Fig. 7C). The top three most common hPTMs that
246 were significantly different in abundance in response to experimental treatments across H2A
247 isoforms were dioxidation (45 significant unique hPTMs), oxidation (38 significant unique
248 hPTMs), and dehydration (25 significant unique hPTMs) (Fig. 7A). Two highly condition-
249 dependent hPTMs were significantly different across six different comparisons: H2A-like
250 (XP_013879560.1) 123K carboxyethylation/lactylation (Figs. 7E, 8B) and H2A-like
251 (XP_013878193.1) 102S dehydration (Figs. 7D, 8C). Two additional highly condition-dependent
252 hPTMs were significantly different across five different comparisons: H2A.V
253 (XP_013854970.1)121K biotinylation and 122K dioxidation (Fig. 9A, Table 2).

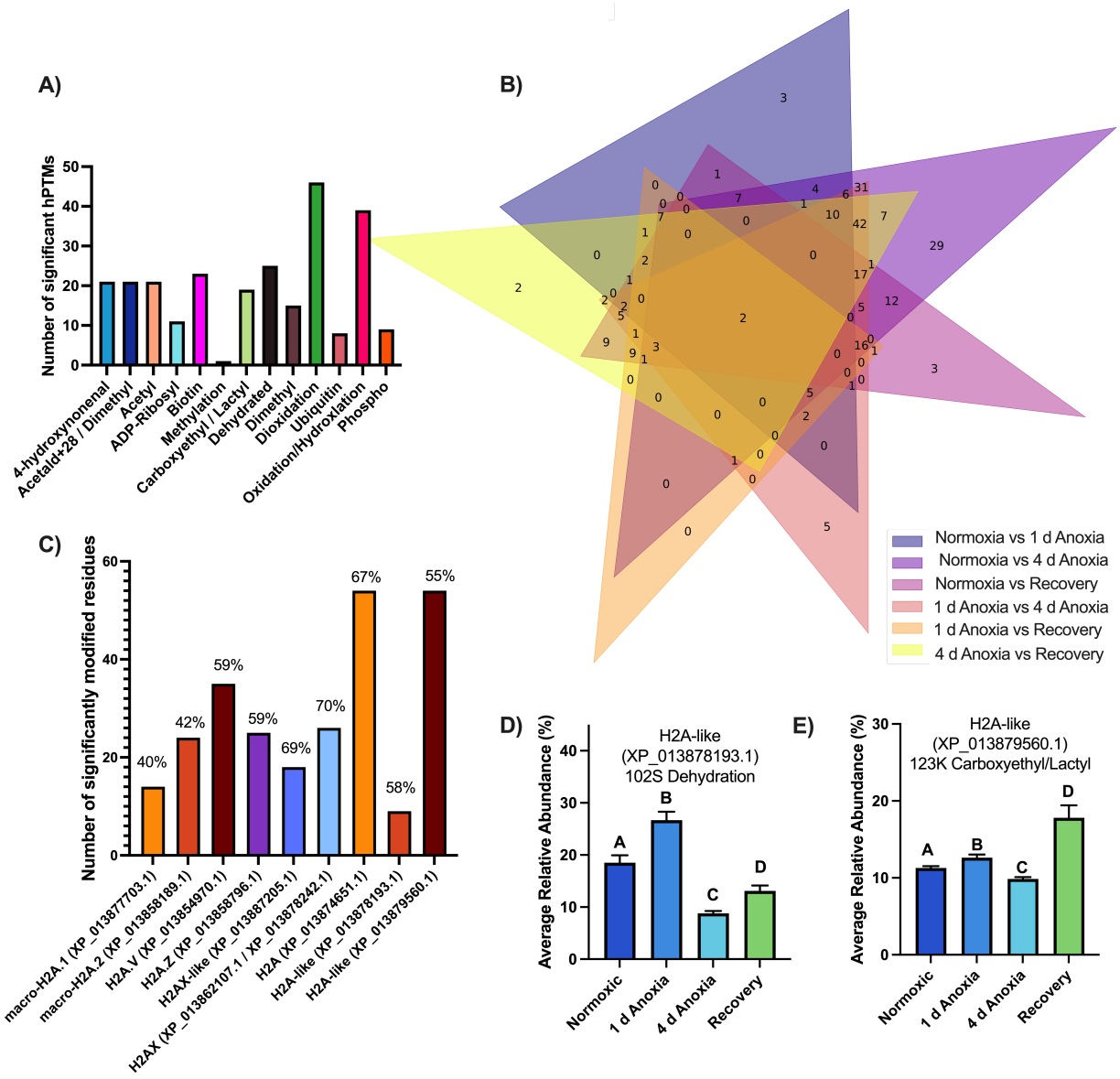

Figure 7. Significant differential post-translational modifications on histone H2A isoforms in WS40NE cells exposed to anoxia and aerobic recovery from anoxia. (A) The top three most commonly significant differential hPTMs across histone H2A isoforms were dioxidation (45 hPTMs), oxidation (38 hPTMs), and dehydration (25 hPTMs). (**B**) Venn diagram illustrating the occurrence of unique and biologically-relevant hPTMs on H2A histone isoforms across experimental treatment groups. (**C**) At least nine H2A isoforms had residues that were significantly modified. The percentage above each bar represents the peptide sequence coverage of that isoform. Note that two isoforms appear to be highly modified based on their percent sequence coverage. Two specific hPTMs were

significant across all six pairwise comparisons: **(D)** H2A-like (XP_013878193.1) 102S dehydration and **(E)** H2A-like (XP_013879560.1) 123K carboxyethylation/lactylation. Bars represent means ± SEM (n=11-12).

Figure 8. Characterization of the post-translational modifications on histone H2A isoforms in WS40NE cells exposed to anoxia and aerobic recovery from anoxia. Isoforms represented are (**A**) H2A (XP_013874651.1), (**B**) H2A-like (XP_013879560.1), (**C**) H2A-like (XP_013878193.1), (**D**) macro-H2A.2 (XP_013858189.1), and (**E**) macro-H2A.1 (XP_0138777031.1). Each panel represents a different amino acid position where at least one hPTM was detected. Amino acid residues are abbreviated using their one letter code. The x-axis displays the condition of the samples: 0 d in anoxia (0), 1 d in anoxia (1), 4 d in anoxia (4), or 1 d of aerobic recovery after 4 days in anoxia

272 (R). The y-axis scales differ across panels to better visualize changes in low abundance hPTMs. Detected (purple)

273 and modified (blue) peptides and the entire peptide sequences are listed beside the panels.

274

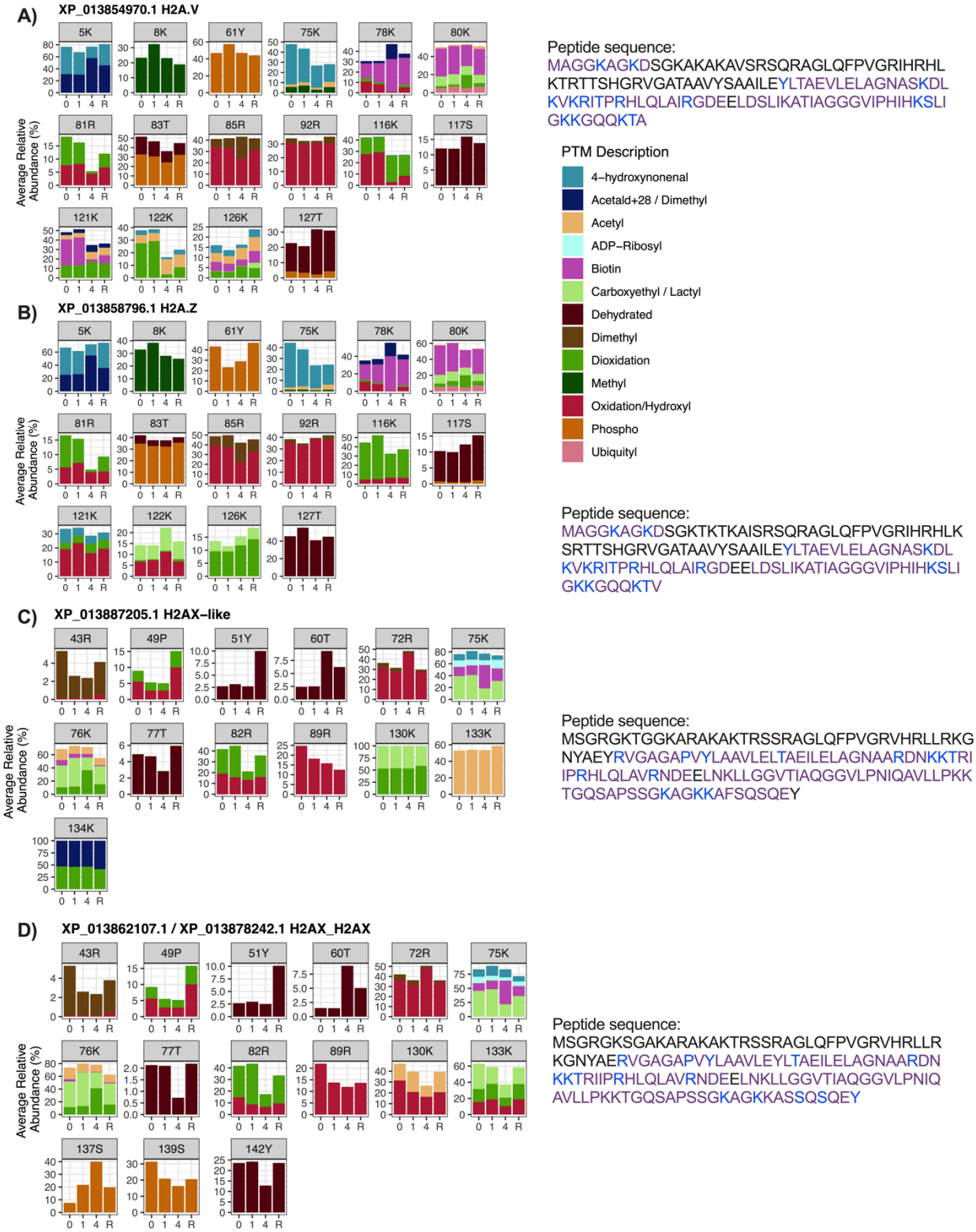
A)
XP_013854970.1 H2A.V
5K
8K
61Y
75K
78K
80K
81R
83T
85R
92R
116K
117S
121K
122K
126K
127T
Average Relative Abundance (%)
0 1 4 R
Peptide sequence:
MAGGKAGKDSGKAKAKAVSRSQRAGLQFPVGRIHRHL
KTRTTSHGRVGATAAVYSAAILEYLTAEVLELAGNASKDL
KVKRITPRHLQLAIRGDEELDSLIKATIAGGGVIPHIHKSLI
GKKGQQKTA
PTM Description
4–hydroxynonenal
Acetald+28 / Dimethyl
Acetyl
ADP–Ribosyl
Biotin
Carboxyethyl / Lactyl
Dehydrated
Dimethyl
Dioxidation
Methyl
Oxidation/Hydroxyl
Phospho
Ubiquityl
B)
XP_013858796.1 H2A.Z
Peptide sequence:
MAGGKAGKDSGKTKTKAISRSQRAGLQFPVGRIHRHLK
SRTTSHGRVGATAAVYSAAILEYLTAEVLELAGNASKDL
KVKRITPRHLQLAIRGDEELDSLIKATIAGGGVIPHIHKSLI
GKKGQQKTV
C)
XP_013887205.1 H2AX–like
43R
49P
51Y
60T
72R
75K
76K
77T
82R
89R
130K
133K
134K
Peptide sequence:
MSGRGKTGGKARAKAKTRSSRAGLQFPVGRVHRLLRKG
NYAEYRVGAGAPVYLAAVLELTAEILELAGNAARDNKKTRI
IPRHLQLAVRNDEELNKLLGGVTIAQGGVLPNIQAVLLPKK
TGQSAPSSGKAGKKAFSQSQEY
D)
XP_013862107.1 / XP_013878242.1 H2AX_H2AX
137S
139S
142Y
Peptide sequence:
MSGRGKSGAKARAKAKTRSSRAGLQFPVGRVHRLLR
KGNYAERVGAGAPVYLAAVLEYLTAEILELAGNAARDN
KKTRIIPRHLQLAVRNDEELNKLLGGVTIAQGGVLPNIQ
AVLLPKKTGQSAPSSGKAGKKASSQSQEY

275

276 **Figure 9. Characterization of the post-translational modifications on histone H2A isoforms in WS40NE cells**
277 **exposed to anoxia and aerobic recovery from anoxia.** (**A**) H2A.V (XP_013854970.1), (**B**) H2A.Z
278 (XP_013858796.1), (**C**) H2AX-like (XP_013887205.1), and (**D**) H2AX-like (XP_013862107.1/ XP_013878242.1).
279 Each panel represents a different amino acid position where at least one hPTM was detected. Amino acid residues
280 are abbreviated using their one letter code. The x-axis displays the condition of the samples: 0 d in anoxia (0), 1 d in
281 anoxia (1), 4 d in anoxia (4), or 1 d of aerobic recovery following 4 d of anoxia (R). The y-axis scales differ across
282 panels to better visualize changes in low abundance hPTMs. Detected (purple) and modified (blue) peptides and the
283 entire peptide sequences are listed beside the panels.

284

285 ***Characterization of histone H2B***

286 At least five H2B proteins were identified: (**A**) H2B_1/2-like (XP_013874662.1), (**B**) H2B_1/2
287 (XP_013879561.1 / XP_013878239.1 / XP_013878163.1 / XP_013869445.1), (**C**) H2B_1/2-like
288 (XP_013857090.1), (**D**) H2B.L4-like (XP_013885354.1), and (**E**) H2B.3-like
289 (XP_013886452.1). Thirteen types of PTMs were identified across these isoforms (Fig. 10A).
290 Three hundred and twenty-seven significant hPTMs were present across H2B isoforms in at least
291 one condition, making this the most significantly modified class of histones in this study (Fig.
292 10B). All identified H2B isoforms had at least one residue with a significant hPTM, while 4 of
293 the 5 were highly modified (Fig. 10C). The top three most commonly significant differential
294 hPTMs across H2B isoforms were phosphorylation (58 significant unique hPTMs), dehydration
295 (49 significant unique hPTMs), and oxidation/hydroxylation (35 significant unique hPTMs) (Fig.
296 10A).The following hPTMs displayed an average relative abundance of exactly 100% in all
297 samples: H2B.L4-like (XP_013885354.1) 31Y, 43T, 46S, and 55S dehydration (Fig. 11, Table
298 1).

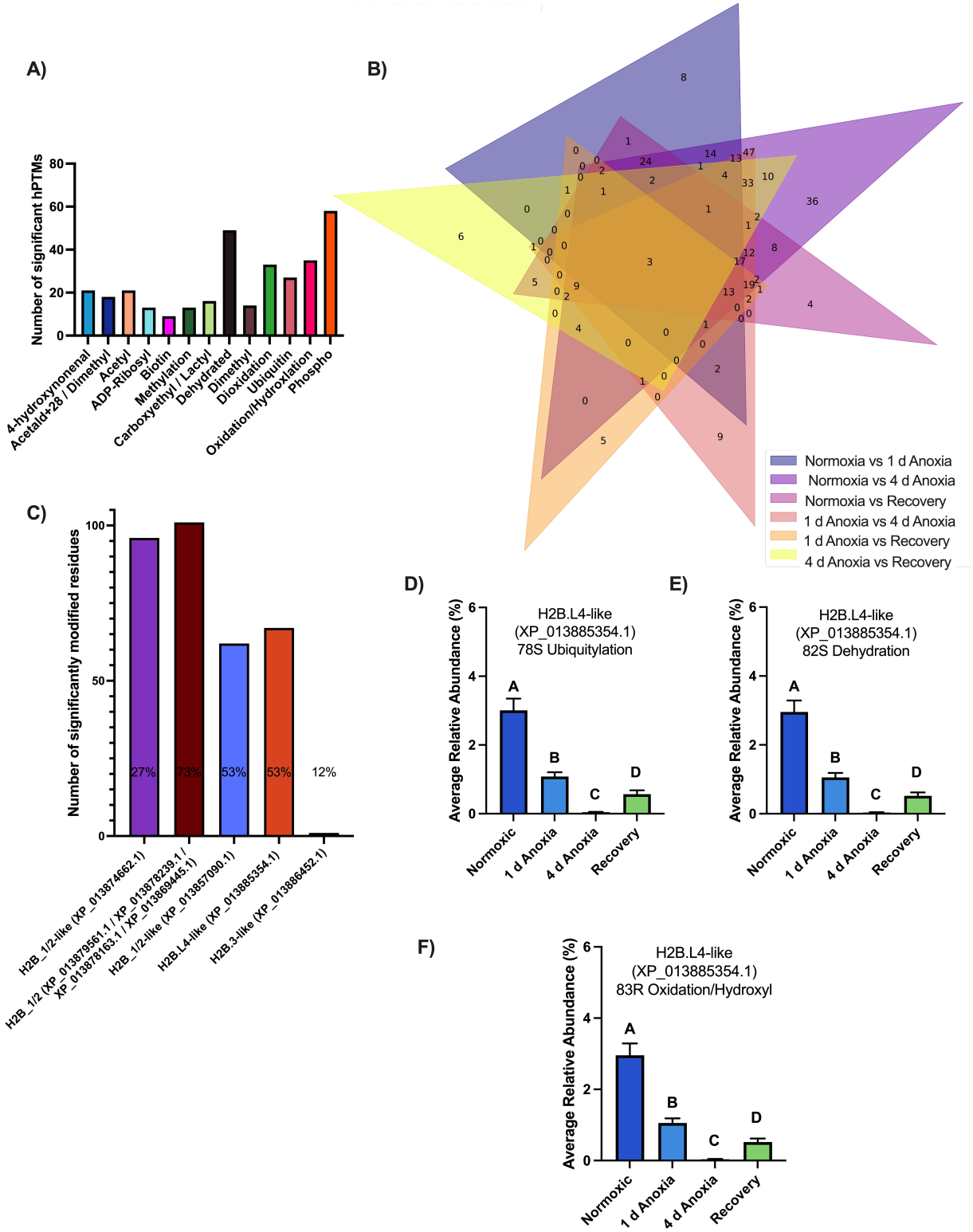

Figure 10. Significant differential post-translational modifications on histone H2B isoforms in WS40NE cells exposed to anoxia and aerobic recovery from anoxia. (A) The top three most commonly significant differential

302 hPTMs across H2B isoforms were phosphorylation (58 hPTMs), dehydration (48 hPTMs), and
303 oxidation/hydroxylation (35 hPTMs). (**B**) Venn diagram illustrating the occurrence of unique and biologically-
304 relevant hPTMs on H2B histone isoforms across experimental treatment groups. (**C**) At least five H2B isoforms had
305 residues with significant hPTMs. The percentage above each bar represents the peptide sequence coverage of that
306 isoform. Three hPTMs on H2B.L4-like (XP_013885354.1) were highly condition dependent across all six
307 comparisons: **(D)** 78S ubiquitylation, **(E)** 82S dehydration, and **(F)** 83R oxidation/hydroxylation. Bars represent the
308 mean ± SEM (n=11-12).

309 Three hPTMs on H2B.L4-like (XP_013885354.1) were highly condition dependent across all six
310 comparisons: 78S ubiquitylation, 82S dehydration, and 83R oxidation/hydroxylation (Fig.
311 10D,E,F). An additional twenty-three hPTMs were highly condition dependent across five
312 different comparisons on four different histone isoforms: eight on H2B_1/2-like
313 (XP_013874662.1), seven on H2B_1/2 (XP_013879561.1 / XP_013878239.1 / XP_013878163.1
314 / XP_013869445.1), four on H2B_1/2-like (XP_013857090.1), and four on H2B.L4-like
315 (XP_013885354.1) (Fig. 11, Table 2). Two of these highly condition-dependent modifications on
316 H2B.L4-like (XP_013885354.1) occur on the same residue: 79T dehydration and
317 phosphorylation (Fig. 11D, Table 2).
318

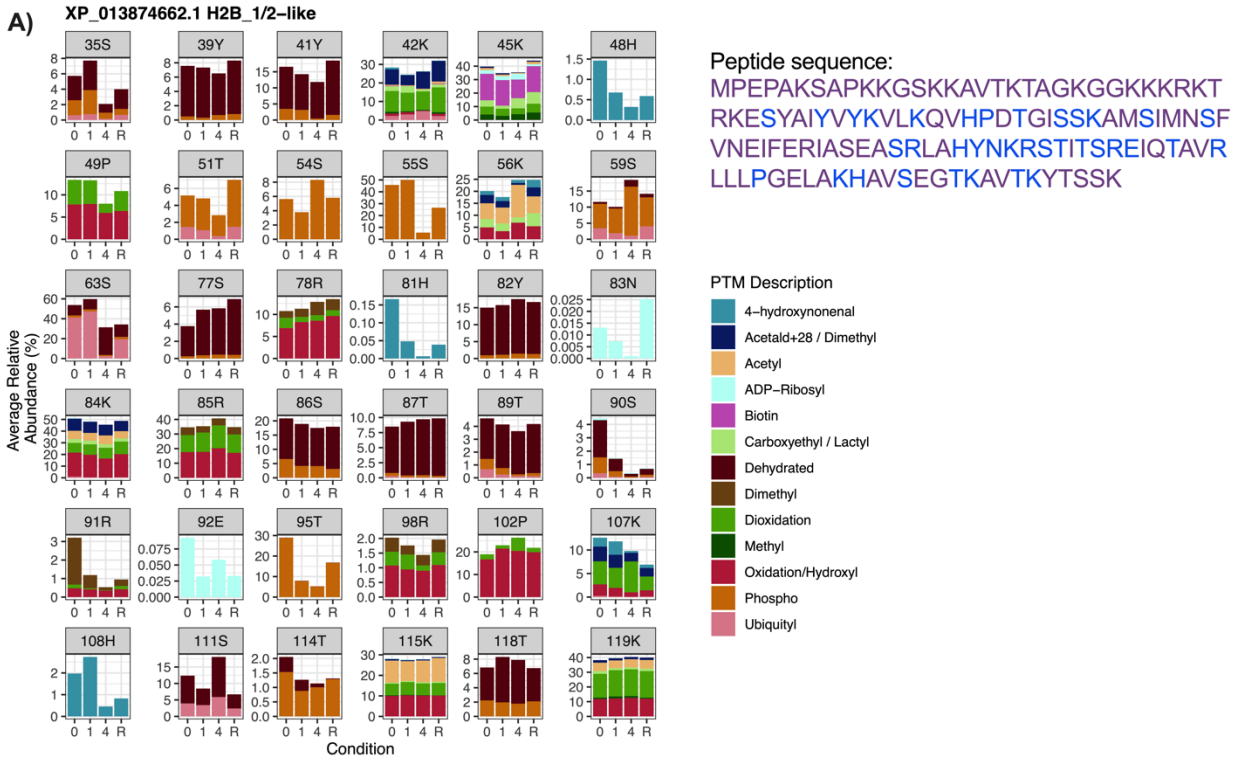
A)
XP_013874662.1 H2B_1/2–like
Average Relative Abundance (%)
Condition
Peptide sequence:
MPEPAKSAPKKGSKKAVTKTAGKGGKKKRKT
RKESYAIYVYKVLKQVHPDTGISSKAMSIMNSF
VNEIFERIASEASRLAHYNKRSTITSREIQTAVR
LLLPGELAKHAVSEGTKAVTKYTSSK
PTM Description
4–hydroxynonenal
Acetald+28 / Dimethyl
Acetyl
ADP–Ribosyl
Biotin
Carboxyethyl / Lactyl
Dehydrated
Dimethyl
Dioxidation
Methyl
Oxidation/Hydroxyl
Phospho
Ubiquityl

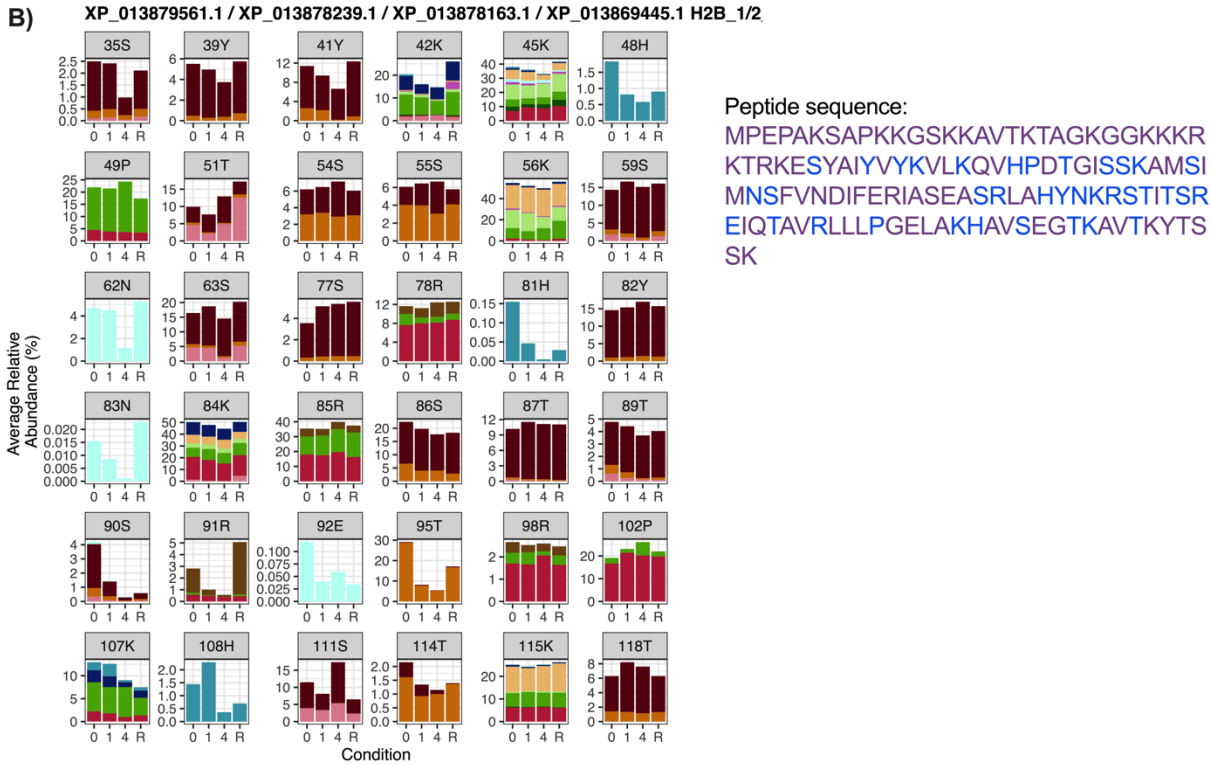
B)
XP_013879561.1 / XP_013878239.1 / XP_013878163.1 / XP_013869445.1 H2B_1/2
Average Relative Abundance (%)
Condition
Peptide sequence:
MPEPAKSAPKKGSKKAVTKTAGKGGKKKR
KTRKESYAIYVYKVLKQVHPDTGISSKAMSI
MNSFVNDIFERIASEASRLAHYNKRSTITSR
EIQTAVRLLLPGELAKHAVSEGTKAVTKYTS
SK

319

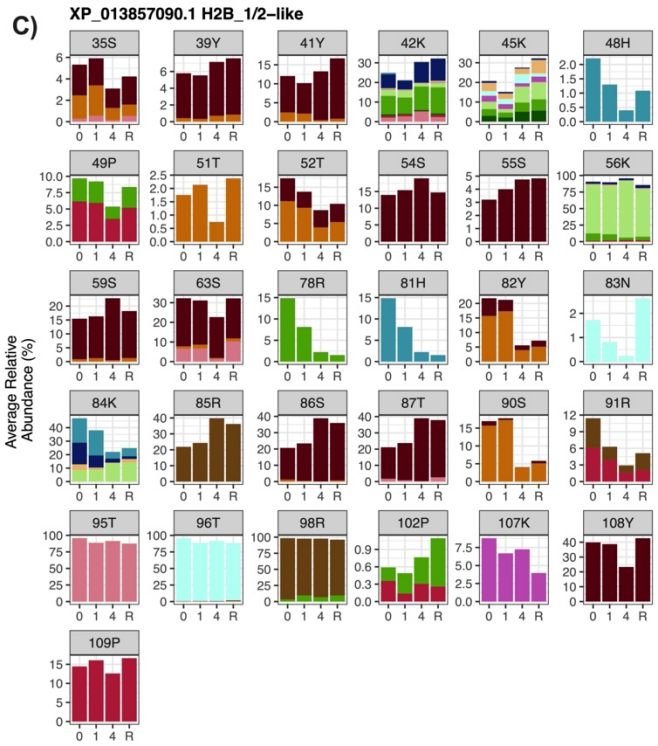

Peptide sequence:
MPEPAKSAPKKGSKKAVTKTAGKGGKKKRKTKKE
SYAIYVYKVLKQVHPDTTISSKAVSFMNSFVNNIFE
RIASKASRLAHYNKRSTITSREIQTTVRLLLPGELA
KYPNN

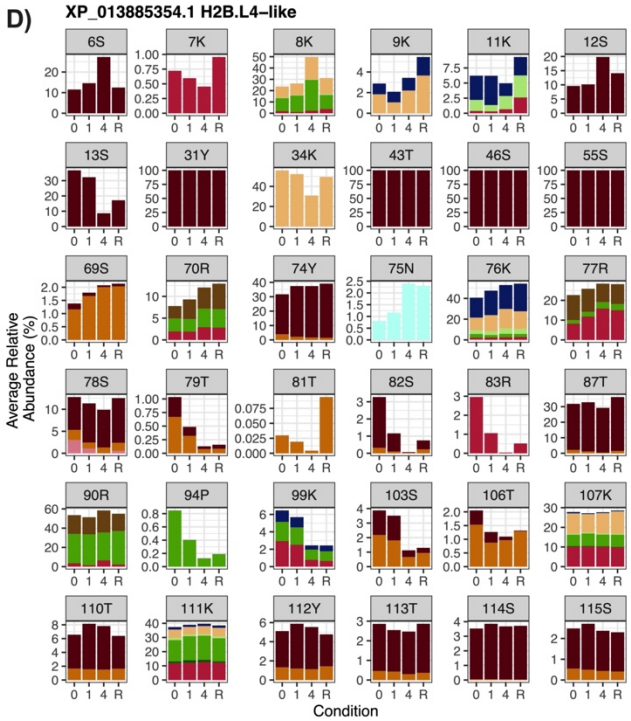

Peptide sequence:
MSNDVSKKKGKSSGDKKAKRKVKRRETYAMYIY
KVLKQVHPDTGISSRAMSIMNSFVNDLFERIATEA
SRLAQYNKRSTITSREVQTAVRLLLPGELAKHAVS
EGTKAVTKYTSSK

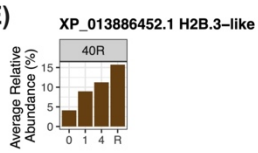

Peptide sequence:
MSIMNSFINIFKRIASKASHLAHYCKRSTITSREIQT
DVRLLLPGELAKHTMSKGTKAXTKYTSSX

320

321

322 **Figure 11. Characterization of the post-translational modifications on histone H2B isoforms in WS40NE cells**
323 **exposed to anoxia and aerobic recovery from anoxia.** Isoforms represented are (**A**) H2B_1/2-like
324 (XP_013874662.1), (**B**) H2B_1/2 (XP_013879561.1/ XP_013878239.1 / XP_013878163.1 / XP_013869445.1), (**C**)
325 H2B_1/2-like (XP_013857090.1), (**D**) H2B.L4-like (XP_013885354.1) and (**E**) H2B.3-like (XP_013886452.1).
326 Each panel represents a different amino acid position where at least one hPTM was detected. Amino acid residues
327 are abbreviated using their one letter code. The x-axis displays the condition of the samples: 0 d in anoxia (0), 1 d in
328 anoxia (1), 4 d in anoxia (4), or 1 d of aerobic recovery after 4 d of anoxia (R). The y-axis scales differ across panels
329 to better visualize changes in low abundance hPTMs. Detected (purple) and modified (blue) peptides and the entire
330 peptide sequences are listed beside the panels.

331 ***Characterization of histone H3***

332 At least three H3 proteins were identified: (**A**) H3.3 (XP_013887037.1 / XP_013885059.1 /
333 XP_013879174.1 / XP_013870443.1), (**B**) H3-like (XP_013879564.1), and (**C**) H3-like
334 (XP_013878241.1). All identified H3 isoforms had at least one residue with a significant hPTM,
335 with 12 types of hPTMs identified across these isoforms (Fig. 12A). The most common hPTMs
336 that differ significantly across experimental treatments on H3 isoforms were
337 oxidation/hydroxylation (23 significant unique hPTMs) and dioxidation (18 significant unique
338 hPTMs) (Fig. 12A). Eighty-nine hPTMs were present across all three H3 isoforms in at least one
339 condition (Fig. 12B). Two hPTMs displayed an average relative abundance of exactly 100% in
340 all samples: H3-like (XP_013878241.1) 17K and 24R oxidation/hydroxylation (Fig. 13C, Table
341 1).

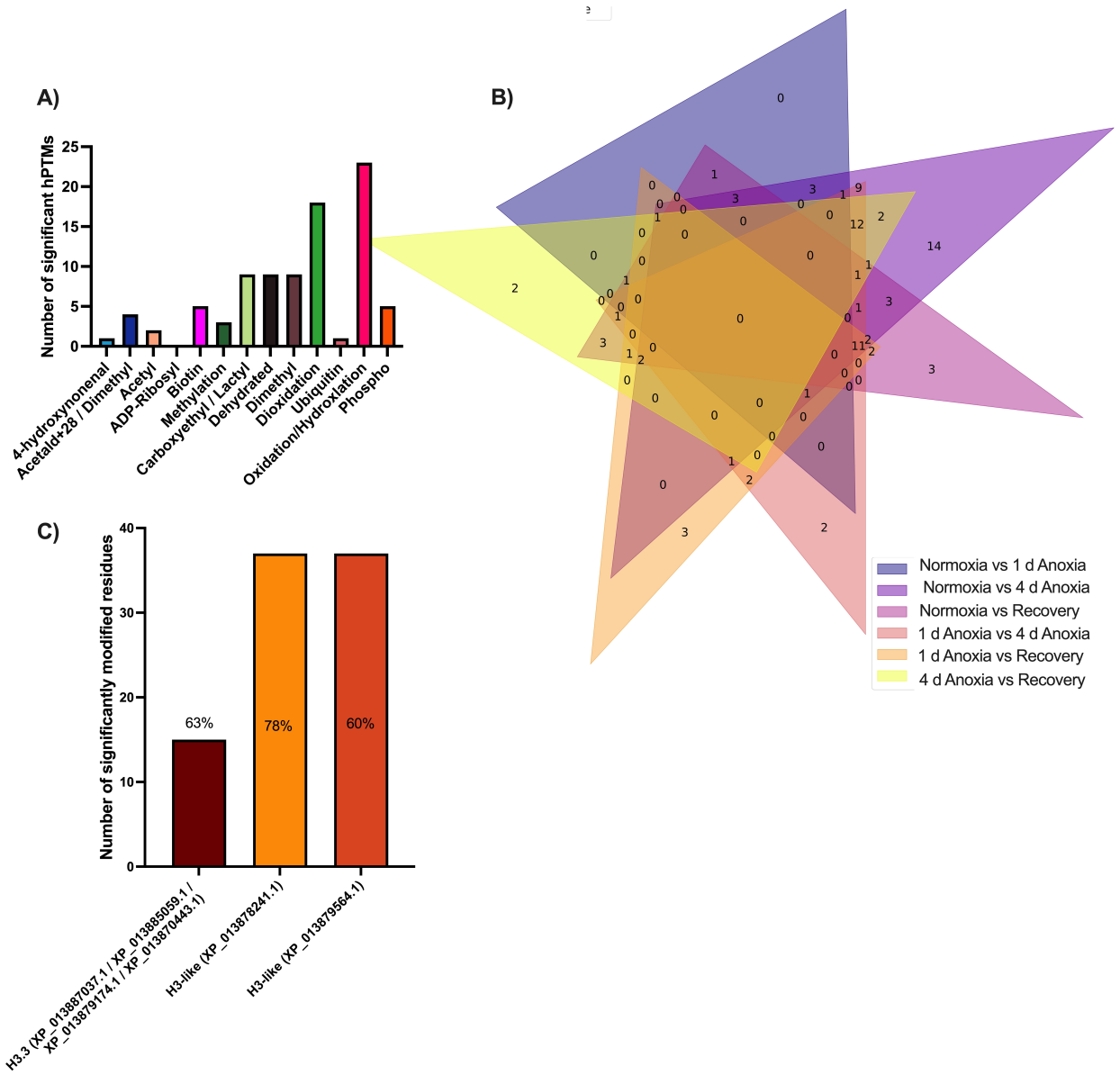

342

343 **Figure 12. Significant differential post-translational modifications on histone H3 isoforms in WS40NE cells**
344 **exposed to anoxia and aerobic recovery from anoxia. (A)** The most commonly significant differential hPTMs
345 across H3 isoforms were oxidation (23 hPTMs) and dioxidation (18 hPTMs). (**B**) Venn diagram illustrating the
346 occurrence of unique and biologically-relevant hPTMs on H3 histone isoforms across experimental treatment
347 groups. (**C**) All identified H3 isoforms had residues with significant hPTM modifications. The percentage above
348 each bar represents the peptide sequence coverage of that isoform. Bars represent the mean ± SEM (n=11-12).

349

Figure 13. Characterization of the post-translational modifications on histone H3 isoforms in WS40NE cells exposed to anoxia and aerobic recovery from anoxia. Isoforms represented are (**A**) H3.3 (XP_013887037.1/

353 XP_013885059.1/ XP_013879174.1 / XP_013870443.1), (**B**) H3-like (XP_013879564.1), and (**C**) H3-like
354 (XP_013878241.1). Each panel represents a different amino acid position where at least one hPTM was detected.
355 Amino acid residues are abbreviated using their one letter code. The x-axis displays the condition of the samples: 0
356 d in anoxia (0), 1 d in anoxia (1), 4 d in anoxia (4), or 1 d aerobic recovery after 4 d of anoxia (R). The y-axis scales
357 differ across panels to better visualize changes in low abundance hPTMs. Detected (purple) and modified (blue)
358 peptides and the entire peptide sequences are listed beside the panels.

359

360

361 ***Extracellular Lactate Accumulation***

362 While previous studies have explored accumulation of lactate during exposure to anoxia in
363 WS40NE cells, this was the first study to monitor how this lactate accumulation persisted during

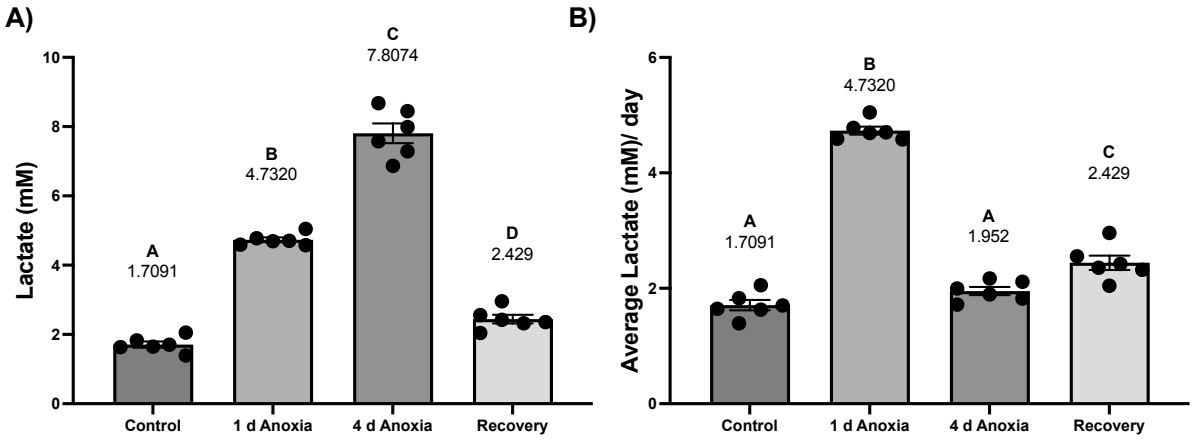

364 recovery (Fig. 14). As previously shown, anoxic WS40NE cells accumulate extracellular lactate
365 at a significantly higher rate than normoxic cells. After 1 d of aerobic recovery, this trend
366 persists.

367 **Figure 14. Extracellular lactate accumulation in WS40NE cells exposed to anoxia and recovery from anoxia.**
368 (**A**) Total media lactate concentration during exposure to anoxia and recovery from anoxia. Due to the recovery
369 media change, the data represents only 1 day of lactate accumulation in normoxic recovery conditions. (**B**) The
370 average rate of lactate accumulation (mM/day) in the same samples. Different letters indicate significant differences
371 in means within each graph (one-way ANOVA with Tukey's HSD test $p > 0.05$, $n = 6$).

372 **Discussion**

373 Histone isoforms and post-translational modifications change in response to anoxia and aerobic
374 recovery from anoxia in WS40NE cells. This is consistent with hypoxic responses in hPTMs and
375 histone isoforms observed in human cells [39, 40]. Significant differences in histone isoform
376 abundance were detected in response to anoxia. Additionally, of the 1043 unique biologically

377 relevant hPTMs detected, 816 hPTMs were significantly modified in at least one condition. All
378 histone groups showed significant post-translational modifications in response to changing
379 oxygen availability. H2B was the most significantly modified histone group with 327 significant
380 differential hPTMs present in at least one condition. H2B_1/2 (XP_013879561.1 /
381 XP_013878239.1 / XP_013878163.1 / XP_013869445.1) was the most significantly modified
382 histone, with 101 significant modifications. Interestingly, highly condition-dependent hPTMs
383 often occurred on adjacent residues, with two highly condition-dependent hPTMs sharing a
384 single residue. This suggests that histones of WS40NE cells have highly modifiable peptide
385 regions that are responsive to changes in oxygen availability and likely help to coordinate
386 changes in gene expression associated with their extreme anoxia tolerance.
387
388 ***Changes in histone isoform abundance***
389
390 Several histone isoforms change in abundance in response to anoxia. While, to our knowledge,
391 no study has identified anoxia-dependent changes in histone isoform abundance, there are
392 several studies that document changes in histone isoforms in response to heat stress, hypoxia,
393 ischemia, and oxidative stress [40-43]. Of note, the increase in histone H3.3 observed in this
394 study is consistent with a role for "priming" the cells for a robust gene expression response to
395 stress as has been shown in human lung fibroblasts [40]. Importantly, histone H3.3 expression
396 responds within 1 day of anoxia and does not immediately return to pre-anoxic levels after 1 day
397 of recovery, suggesting a prolonged change in poise of the chromatin. H3.3 is typically
398 associated with euchromatin and active regulatory elements [44], suggesting that the genomic
399 location of the histone H3.3 isoforms may indicate genes that are immediately responsible for

400 supporting cellular functions in the absence of oxygen, or may represent genes primed and ready
401 to be expressed during recovery from anoxia. If future studies can identify the genomic location
402 of the H3.3 isoforms, these genes would be prime candidates for explaining anoxic-
403 preconditioning in embryos of *A. limnaeus* [45].
404
405 H2A/H2B dimers flank entry and exit portals for DNA in the nucleosome, and thus changes to
406 these histone isoforms are highly likely to impact gene expression [46, 47]. In WS40NE cells,
407 one histone H2A isoform decreases within 1 day of anoxia, while two histone H2B isoforms
408 decrease, but only after 4 days of anoxia, suggesting unique regulation and usage of these
409 isoforms in response to anoxia. Histone H2A isoforms have been shown to increase after
410 exposure to hypoxia and ischemia in some mammalian models [48, 49], a result that is opposite
411 of that in WS40NE cells. The reason for this shift and their potential for altering gene expression
412 is worthy of future studies.

413 **Global patterns of histone ubiquitylation in WS40NE cells exhibit similar patterns to whole**
414 **embryos**

415 The global decrease in histone ubiquitylation during anoxia reported here supports earlier work
416 on whole embryos of *A. limnaeus* [50]. WS40 embryos (the stage of embryo that WS40NE cells
417 were isolated from) exhibit a global decrease in ubiquitin conjugates after 3 days of anoxia that
418 return to pre-anoxic levels after 1 day of aerobic recovery [50]. Interestingly, a ubiquitylated 23
419 kDa protein, hypothesized to be a histone, in these embryos was absent during anoxia and
420 present only when oxygen was available. In the residue-specific data presented here, only one
421 residue fits this pattern: serine 63 on H2B-1/2-like (XP_013874662.1) decreases from 41.3%
422 ubiquitylated in normoxia to 2.3% after 4 days of anoxia. A similar pattern on the same serine

423 residue is observed in another H2B-1/2-like isoform (XP_013857090.1), but on this isoform the
424 residue has a much lower rate of modification and instead is dominated by dehydration. Thus,
425 antibody- and MS-based data suggest a possible role for this ubiquitylation in managing gene
426 expression in response to long-term anoxia. However, it should be noted that different stage
427 embryos illustrated different patterns, with developing embryos that exhibit extreme anoxia
428 tolerance (WS36 embryos) accumulating ubiquitin conjugates only after 1 d of aerobic recovery
429 from long-term anoxia [50]. Future work should be done to elucidate the complex nature of the
430 ubiquitin system in both WS40NE cells and *A. limnaeus* embryos, particularly in understanding
431 the role of histone ubiquitylation in anoxia.

432 ***Global decreases in multiple hPTMs deviate from expected patterns***

433 Global changes to hPTMs have been recorded in mammalian cells in response to hypoxia; large
434 changes in modifications of H3 and H4 histones are seen in HEK 293T, HeLa and RKO cells
435 with smaller changes occurring on H2A and H2B histones [39]. However, few studies have
436 investigated anoxia-induced changes in hPTMs in a modification-specific way [34].
437 Interestingly, global methylation in WS40NE cells is stable for the first day of anoxia, but then
438 significantly decreases during 4 d anoxia and remains low for 1 d of aerobic recovery. As
439 H3K4me3 and H3K36me3 increase within 1 h during hypoxia in mammalian systems, we
440 expected global methylation in *A. limnaeus* to reflect similar changes [28]. Increases in
441 methylation in hypoxic mammalian systems is thought to be due to decreased activity of histone
442 demethylases when oxygen is limiting, mainly because many of these enzymes use molecular
443 oxygen as a substrate, and at least one histone demethylase appears to be upregulated in a
444 hypoxia-inducible factor dependent manner, presumably to combat the overall loss of
445 demethylase activity during hypoxia [51]. Thus, the large and sustained decrease in global

446 methylation exhibited in killifish WS40NE cells is an unexpected result when referenced to the
447 mammalian literature. Histone methylation, including di- and trimethylation, is associated with
448 transcriptional activation and repression in a residue specific manner [52, 53], so it is difficult at
449 this time to draw any conclusions for the role that decreased methylation might play. Of note,
450 only one site of methylation in our dataset was highly condition dependent (H2B_1/2,
451 XP_013874662.1 and XP_013869445.1, 124K). This residue does not correspond with any
452 known mammalian hPTMs but may serve a similar function and should be investigated further.

453 Given its role in the regulation of DNA repair [54], it is surprising that global levels of ADP-
454 ribosylation consistently decrease in anoxia and remain depressed during aerobic recovery. Most
455 residue-specific patterns match this global pattern with either stable or decreasing levels of ADP-
456 ribosylation during anoxia. However, in the cases where an increase occurs on a specific residue,
457 it is almost always during aerobic recovery. This suggests a conserved role for ADP-ribosylation
458 of histones associated with oxidative stress and the DNA damage response [54, 55]. However,
459 PARPs including diphtheria-toxin-like ADP-ribose transferases (ARTDs) and cholera-toxin-like
460 ARTCs can modify a variety of residues: lysine, aspartate, glutamate, serine, arginine, tyrosine,
461 and histidine [56, 57]. Additionally, ADP-ribosylation can occur on arginine, serine, threonine,
462 and cysteine residues via the action of sirtuins (SIRT4, SIRT6, and SIRT7) that perform mono
463 (ADP-ribose) (MAR) addition [56]. Histone ADP-ribosylation is associated with a variety of
464 functions beyond DNA damage response, including chromatin remodeling and facilitation of
465 gene transcription by making chromatin more accessible [58, 59]. A decrease in ADP-
466 ribosylation may be associated with a decrease in chromatin availability, decreasing the
467 accessibility of the genome to polymerases and transcription factors. Thus, the overall decrease

468 in histone ADP-ribosylation may support the downregulation of transcription associated with
469 entrance into anoxia-induced quiescence.

470 Recent studies suggest lactate accumulation in mammalian cells may play a role in cell signaling
471 and regulation through histone lactylation [60], including stimulating gene transcription in
472 macrophages [61]. WS40NE cells accumulate extracellular lactate throughout anoxia and during
473 at least the first day of aerobic recovery. Lactate is a glycolytic end-product that has classically
474 been considered an unavoidable consequence of vertebrate anaerobic metabolism, but in
475 WS40NE cells, 49 unique carboxyethylation/lactylation modifications significantly changed in
476 abundance in at least one comparison and one of these modifications was classified as highly
477 condition dependent (Table 2). Surprisingly, increased lactate accumulation in WS40NE cells is
478 correlated with *decreased*, not increased, global carboxyethylation/lactylation. This pattern is the
479 opposite of what is seen in human MCF-7, HeLa, and MDA-MB-231 cells, which demonstrate a
480 dose-dependent increase in histone lactylation in response to 25 mM exogenous L-lactate [61].
481 On a residue-specific level there are 70 residues with carboxyethylation/lactylation present, and
482 one of these residues is highly condition dependent. Given the extreme rarity of protein
483 carboxyethylation, these are most likely sites of lactylation [62]. In almost all cases, residues in
484 WS40NE histones experience a decrease in lactylation during anoxia. It is possible that the
485 slower rate of lactate accumulation in WS40NE cells (7.8 mM extracellular lactate after 4 days
486 of anoxia) does not produce enough lactate to cause increase lactylation. However, lactate levels
487 are relatively low during normoxia, and yet many histone residues still have a high percentage of
488 lactylation. Thus, it would seem that lactate availability is not likely to limit histone lactylation in
489 WS40NE cells. It is worth considering that decreased rates of lactate accumulation and decreased

490 histone lactylation in WS40NE cells may at least partially underlie their extreme anoxia
491 tolerance, as this is contrary to trends that appear in anoxia intolerant mammalian cells.

492 ***Several hPTMs suggest protection against ROS damage***

493 Stress related hPTMs, including oxidation/hydroxylation and dioxidation, increase globally in
494 response to anoxic stress and aerobic recovery in WS40NE cells. This increase is expected, as
495 these hPTMs are known to increase during stress due to increased rates of reactive oxygen
496 species (ROS) production [63, 64]. While oxidation of proteins can be the result of nonenzymatic
497 ROS damage, several enzymes are involved in histone hydroxylation and oxidation [65-67].
498 Jumonji domain containing 6 (JMJD6) protein is known to hydroxylate histone lysine residues
499 while the lysyl oxidase (LOX) family of proteins are able to oxidize histone lysines [65, 66].
500 These enzymes may be interesting targets of future work in the WS40NE cell line, because a
501 number of specific residues defy the global pattern and decrease in response to anoxia, while
502 others remain stable, suggesting an enzymatic mechanism and not oxidative damage. Given the
503 role of prolyl-hydroxylases in regulating oxygen-dependent gene expression, investigating
504 histones that decrease in oxidation in response to anoxia (e.g., H3-like, XP_013879564.1, 196R)
505 may hold promise for finding histone oxygen sensors that could participate in regulation of gene
506 expression at the local level.

507 Unexpectedly, another stress related hPTM, 4-hydroxynonenal (4-HNE), remains stable for the
508 first day of anoxia and then significantly decreases after 4 days of anoxia. This decrease
509 continues during the initial 1 day of aerobic recovery. 4-hydroxynonenal is a product of lipid
510 peroxidation, and therefore its presence would be expected to increase with ROS stress [68], as
511 would be expected during both the transition into and out of anoxia. Fish, however, are known to

512 have high levels of antioxidants that mediate ROS stress and allow them to maintain low levels
513 of lipid peroxidation [69, 70]. In addition, embryos of *A. limnaeus* have an extremely high level
514 of antioxidant capacity [71]. Thus, it is possible that WS40NE cells have a mechanism to prevent
515 lipid peroxidation during anoxia.

516 ***Dehydration and phosphorylation – a reciprocal relationship?***

517 Dehydration, especially of serine, threonine, and tyrosine, increases globally in response to
518 anoxic stress and aerobic recovery in WS40NE cells. In addition, some histone isoforms contain
519 stable and apparently permanent dehydrations, suggesting functional importance and a likely
520 enzymatic synthesis of this PTM. Amino acid dehydration is an elimination reaction that results
521 in a dehydroamino acid through the removal of a hydroxyl group [72] or by the direct removal of
522 a phosphate group [73]. On residues S and T, it is specifically a beta-elimination that results in
523 production of dehydroalanine [74]. Dehydroalanine, though common in bacterial and fungal
524 models, is considered rare in mammals [75, 76]. However, to our knowledge, dehydroamino
525 acids, including dehydroalanines, have not been investigated in context of fish models.
526 Additionally, dehydration resulting in dehydroalanines has not been well described as a hPTM,
527 although it has been described as an intermediary PTM in the maturation of lanthipeptide
528 antibiotics [72], and as a PTM in microbially-catalyzed modification of eukaryotic kinases [73].
529 In the case of kinase modification, microbial enzymes, such as phosphothreonine lysases, can
530 target specific MAP kinases and dehydrate residues that would normally be phosphorylated,
531 leading to inactivation and signaling dysregulation [73]. An enzyme responsible for dehydration
532 of these amino acids (S and T) would be needed to support this potential mechanism in WS40NE
533 cells, but it remains unknown. While no specific candidate enzyme has been identified, it is

534 interesting that eukaryotic genomes contain LanC-like proteins that share sequence and structural
535 similarity to bacterial proteins involved in the synthesis of lanthipeptides [73].

536 Dehydration of residues in WS40NE cell histones increases globally, while conversely, global
537 phosphorylation decreases during anoxia and aerobic recovery from anoxia. These patterns are
538 surprising, and the apparent reciprocal patterns of abundance are potentially very interesting.
539 Stress-induced phosphorylation of specific H3 residues is described in mammalian cells (10S and
540 11T), although these specific residues were not captured in our dataset [77]. Nevertheless, we
541 hypothesize that histone dehydration may be a protective feature that prevents inappropriate
542 phosphorylation of specific residues. Competition between dehydration and phosphorylation
543 appears to be particularly present on two canonical H1 isoforms (XP_013879563.1 and
544 XP_013855658.1) in our dataset. Phosphorylation of H1 in response to anoxia is understudied;
545 however, global dephosphorylation of mammalian H1 is documented to occur after induction of
546 apoptosis [78]. In WS40NE cells, H1 residues show various patterns of modifications. For
547 example, the relative abundance of XP_013855658.1 59Y phosphorylation remains stable in
548 anoxia but the relative abundance of dehydration increases. Conversely, XP_013855658.1 46S
549 phosphorylation increases in anoxia while dehydration decreases. These unique response patterns
550 at different residues suggest a residue-specific mechanism may lead to changes in
551 phosphorylation and dehydration at specific H1 sites. Other residues not captured by our
552 methodology should also be investigated for dehydration and phosphorylation competition. For
553 example, in mammalian cells, phosphorylation of H2B 14S is associated with apoptosis and is a
554 documented response to hypoxia [77, 79]. This residue best corresponds to 12S (13S if the first
555 methionine is counted as residue 1) in *A. limnaeus* [34], and was unfortunately not captured in

556 the dataset. Dehydration of this residue could be a possible mechanism for preventing apoptosis
557 and deserves future investigation.

558 One important site of phosphorylation was detected in WS40NE histones: H2A.X 137S.
559 Phosphorylation of mammalian 139S (γ–H2A.X) initiates the DNA repair response and would
560 therefore be expected to increase during anoxia due to an increase in ROS [80]. Surprisingly,
561 137S, the equivalent residue in WS40NE histone H2A.X, experiences a decrease in
562 phosphorylation by 1 day in anoxia and continues to decrease during 4 days of anoxia.
563 Interestingly, a nearby dehydrated residue, 142Y, follows the opposite pattern, increasing during
564 anoxia. In this dataset, phosphorylation never occurs at this tyrosine residue. This is unexpected,
565 as constitutive phosphorylation of mammalian 142Y by Williams–Beuren syndrome
566 transcription factor (WSTF) occurs during normal conditions while dephosphorylation of this
567 site occurs during the DNA damage response [81]. This dephosphorylation has been theorized to
568 enhance recruitment of protein kinases to better maintain γ–H2A.X phosphorylation [81].
569 Therefore, it is interesting that this site is dehydrated, as these dehydrations may prevent
570 phosphorylation and thus prevent the dampening of the DNA damage response that is observed
571 in mammalian cells [81]. These sites should be explored in the future, as they are implicated in
572 regulation of transcription and may have nearby sites of dehydration that are involved in their
573 modification status [82].

574 ***Multiple hPTMs do not return to baseline after 1 day aerobic recovery***

575 The histone landscape of WS40NE cells remains altered after 1 day of aerobic recovery from 4
576 days of anoxia. Which is still considered a relatively short duration of anoxia given that the cells
577 can survive for 49 days without oxygen [37]. Globally, 8 of the 13 types of hPTMs detected are

578 significantly different in recovery compared to normoxia. Based on the $\log_2$ fold-change, global
579 acetylation, oxidation/hydroxylation, and dioxidation are significantly elevated during recovery
580 while global phosphorylation, biotinylation, 4-hydroxynonenal, methylation, and
581 carboxyethylation/lactylation are all decreased. Of the unique hPTMs that were significantly
582 modified, 42% are associated with recovery. While many of the hPTMs may simply not have
583 returned to baseline, other modifications may be involved in recovery mechanisms. Further work
584 will need to be done to determine if these hPTMs return to normoxic levels, or if they represent
585 potential heritable epigenetic alterations to the histone landscape and act as a cellular memory of
586 past exposures to anoxia.

587 **Conclusion**

588 WS40NE cells are unique in their ability to survive long bouts of anoxia and demonstrate
589 changes in their histone landscape in response to different lengths of time in anoxia and recovery
590 from anoxia. This response includes altering both histone isoform relative abundance and hPTM
591 relative abundance at multiple amino acid positions. This response likely contributes to the
592 anoxia tolerance displayed in this cell type. Downstream effects of specific hPTM changes
593 should be studied in the future to determine how specific hPTMs can impact gene expression and
594 anoxia tolerance. Of specific interest is the potential reciprocal relationship between dehydration
595 and phosphorylation as a regulatory mechanism to alter gene expression in response to anoxia.
596

597 **Methods**

598 ***WS40NE Cell Maintenance and Anoxic Exposure***

599 Cells were grown in cell culture media (L-15 + 8.5% FBS, 5 mM glucose, 100 U/mL penicillin/
600 streptomycin) in 100 × 20 mm tissue culture dishes at 30°C and split when confluent using
601 TrypLE Express [37]. For all anoxic experiments, plates of cells were seeded at 2.5 x 10^6 cells
602 per plate and given 24 h to adhere. Cells were then introduced into an anoxic chamber (Bactron
603 EZ, Sheldon Manufacturing, Cornelius, OR, USA) that contains an atmosphere of 95% N_2 and
604 5% H_2. Media was immediately replaced with anoxic media that had been purged with N_2 gas for
605 30 min and then pre-equilibrated to the atmosphere of the anoxic chamber overnight. Cells were
606 harvested at **A)** 0 h of anoxia (normoxic), **B)** 1 d of anoxia, **C)** 4 d of anoxia, and **D)** after 1 d of
607 aerobic recovery following 4 d of anoxia (n = 12). To harvest, media was removed and a cell
608 scraper was used to gently dissociate cells from the bottom of the plate. Two 100 × 20 mm tissue
609 culture dishes were pooled for each replicate. Cell pellets were generated by subjecting the
610 isolated cells to centrifugation at 500 x *g* for 7 min at 4° C, and removing the supernatant.
611 Additionally, media samples were taken directly prior to the harvest of all four timepoints and
612 used to determine the levels of extracellular lactate accumulation. Cell pellets and spent media
613 were flash frozen in liquid nitrogen. Samples were stored at -80° C until use for histone acid
614 extraction or determination of lactate concentration.

615 ***Histone Acid Extraction and Protein Digestion***

616 A middle-down approach to proteomics was used for liquid chromatography mass spectrometry
617 (LCMS) using previously described methods [34, 83]. Histone acid extracts were generated by
618 resuspending cell pellets in 0.4 N H_2SO_4 and incubating the samples with constant rotation at 4
619 °C for 4 h. Samples were then centrifuged at 16,000 x *g* for 10 min at 4 °C and the supernatant
620 was transferred into a fresh 1.5 mL tube. This process was repeated twice. Trichloroacetic acid

621 (TCA) was added to each sample drop-by-drop until a volume equal to 25% of the estimated
622 sample volume had been added. Samples were inverted to mix and incubated overnight at 4 °C.
623 Once the histone proteins had precipitated, samples were centrifuged at 3,400 x *g* for 5 min at 4
624 °C, and the supernatant was discarded. The remaining pellet was rinsed twice: first in ice cold
625 acetone with 0.1% hydrochloric acid and then with 100% acetone. For both rinses, the samples
626 were centrifuged at 3,400 x *g* for 2 min at 4 °C and the supernatant was removed. After both
627 rinses were complete, histone pellets were air dried in a fume hood for 5 min. Samples were
628 stored at -80 °C until the in-solution digestion.
629
630 To begin the digestion, each sample was brought to room temperature (RT), and the histone
631 pellet was resuspended in 138 µL of 8 M urea. Dithiothreitol (DTT) was added to a final
632 concentration of 10 mM. Each sample was then briefly vortexed, centrifuged, and incubated at
633 37 °C for 30 min. Iodoacetamide (IAA) was added to each sample to a final concentration of 30
634 mM, and samples were briefly vortexed and centrifuged before a 30 min incubation in the dark at
635 RT. Samples were briefly vortexed and centrifuged again after the incubation and protein
636 concentration was determined through a bicinchoninic acid (BCA) assay, (cat# 23250, Thermo
637 Scientific, Waltham, MA, USA). Each sample (50 µg of total protein) was diluted 5:6 (v:v) in
638 0.1M sodium phosphate buffer (pH 7.8). V8 protease beads (cat#20151, Thermo Scientific,
639 Waltham, MA, USA) were added at 1:50 ratio (protease:total protein). In sodium phosphate
640 buffer, V8 protease cleaves proteins at the carboxyl end of both glutamate and aspartate residues.
641 After a 20 h incubation with constant rotation at 30 °C, protease beads were removed by
642 centrifugation at 500 x *g* for 2 min and the supernatants were retained. Supernatants were
643 subjected to an additional centrifugation at 19,000 x *g* for 5 min, and those subsequent

644 supernatants were transferred to fresh tubes and dried using a SpeedVac (Thermo Savant,
645 model# ISS110, Thermo Scientific, Waltham, MA, USA). The peptide pellets were reconstituted
646 to a final concentration of 333 ng/µL in 0.1% formic acid diluted in LCMS-grade water. For
647 peptide clean-up, Pierce C18 Spin Columns (cat# 89873, Thermo Scientific, Waltham, MA,
648 USA) were used according to the manufacturer's instructions.
649
650 Data-dependent acquisition (DDA) was used to generate peak lists [84], and PEAKS Suite X
651 Plus and MSFragger to annotate histone peptides using the *A. limnaeus* reference proteome [85].
652 Data-independent acquisition (DIA) was then used to quantify the peptides in the samples.

653 ***Lactate Accumulation Assay***

654 Lactate concentration in the cell culture media was measured enzymatically as previously
655 described [37]. Briefly, each well of a 96-well plate (black walls, clear bottom, Greiner Bio-One,
656 Monroe, NC, USA) contained the following enzyme assay cocktail: 218 µL of Glycine (0.6 M)-
657 Hydrazine (0.5 M) buffer (pH = 9.2), 25 µL 27 mM NAD^+ , 5 µL of lactate standard or sample,
658 and 2.5 µL lactate dehydrogenase (LDH, 14 U/mL, Sigma Aldrich). Change in absorbance was
659 measured at 340 nm every min for 60 min using a plate reader (Tecan Infinity M200Pro,
660 Männendorf, Switzerland). Final concentration of lactate in the samples was determined by
661 interpolation using a lactate standard curve.

662 ***Histone and hPTM Library Generation***

663 Peptides modified with hPTMs were distinguished from unmodified sequences based on their
664 mass shift (Fig. S1). A list of histone PTMs was compiled according to the histone protein name,

amino acid residue/position, and modification type using Python code as previously described [34]. All histone PTMs detected were evaluated for their biological relevance (classified as post-translational, other, or multiple) according to their Unimod accession and amino acid residue. Modifications classified by Unimod as known artefacts or chemical derivatives were removed from analysis. Modifications with the same mass shift are listed together. Peptides that mapped to multiple histones in the *A. limnaeus* genome are presented as a protein family and are reported together.

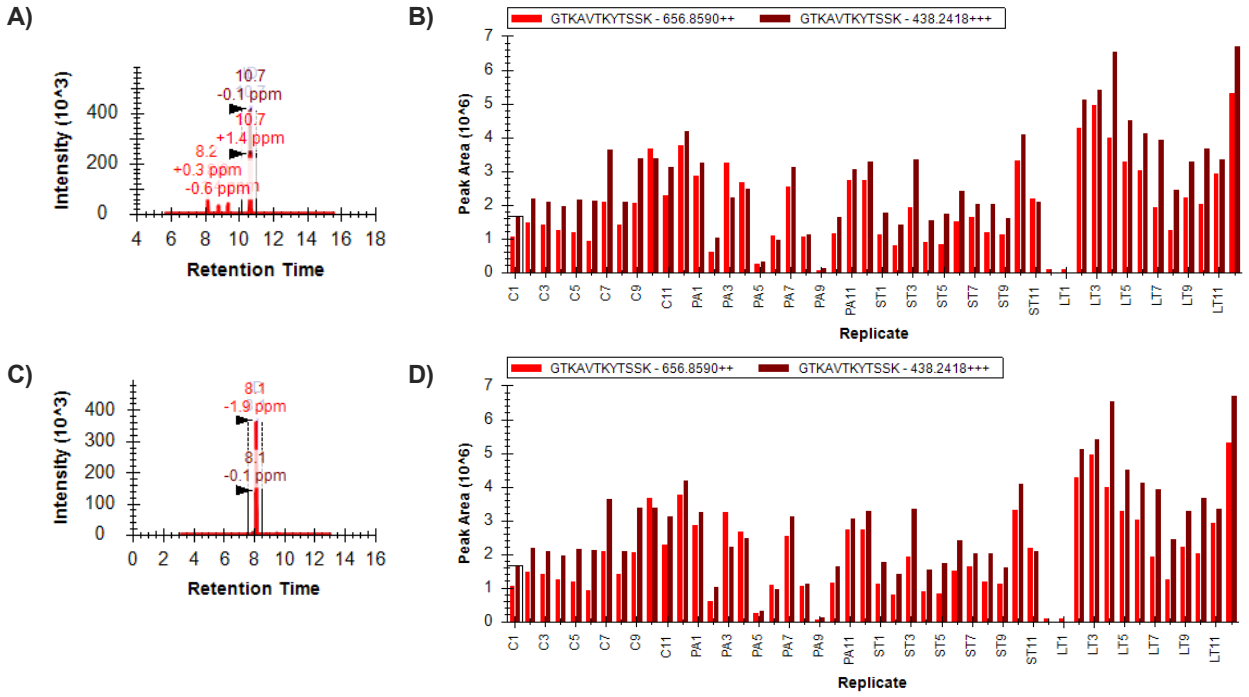

Figure S1: Quantification of histone post-translational modifications in Skyline. A representative MS spectrum (**A**) and peak area (**B**) of the most abundant ions for a modified peptide, E.GTK[+42]AVTKYTSSK, and **(C,D)** the corresponding unmodified peptide E.GTKAVTKYTSSK. A mass shift of +42 on a peptide represents acetylation.

Protein Abundance and hPTM Statistical Analyses

677 Histone isoform abundance was evaluated using quantile normalized raw protein abundance data
678 in Python as previously described [34]. Principal component analysis (PCA) and two-tailed t-
679 tests with the Benjamini-Hochberg correction applied to account for multiple hypothesis testing
680 [86] were used to make inferences about histone isoform abundance.

681 Peptide abundance, as determined by normalized area under the curve, and raw protein
682 abundance were obtained using Skyline (Version 22.2) [87]. Relative abundance values were
683 used to calculate beta-values and M-values. Beta-value is a transformation of relative abundance
684 expressed as a number between 0 and 1 calculated by adding a value of 100 to the denominator
685 to standardize low intensity peptides [88]. The M-value is a logit transformation of the beta-
686 value [89]. Additionally, the relative abundance of each hPTM was used to calculate the $\log_2$
687 fold change, and a two-tailed t-test was used to compare the relative abundance of hPTMs in all
688 conditions with the Benjamini-Hochberg correction applied to account for multiple hypothesis
689 testing [86]. This relative abundance analysis was repeated to analyze global hPTM levels and
690 calculate the $\log_2$ fold change. Additionally, an ANOVA was performed on the global relative
691 abundance of each hPTM using Prism (ver 10.0.0, GraphPad, Software, Boston, MA, USA). A
692 Dunnett's multiple comparison test was used to determine significance of all conditions
693 compared to normoxia. The global relative coverage of each modifiable amino acid residue was
694 calculated to determine what percentage of each hPTM was present at each modifiable residue.

695 Histone PTM maps were constructed for anoxic and normoxic samples using the mean relative
696 abundance of hPTMs. The M-value was used to perform a principal component analysis (PCA).
697 All abundance plots and PCA plots were made in R using the package ggplot2 [90]. Global
698 hPTM abundance, protein relative abundance, and global relative residue coverage were
699 visualized using Prism (ver 10.0.0, GraphPad, Software, Boston, MA, USA). All Python and R

code is accessible by the public on GitHub at https://github.com/hughcj11/WS40NE_Histone_PTM_Analysis. Supplementary data including average relative abundance, t-statistic, p-value, and corrected p-value is provided for each unique, biologically relevant hPTM are provided in Supplementary Table S1 (Excel workbook) across all aerobic conditions.

Author Contributions

JEP and CH conceived and designed the study. CH and EAM performed the experiments and acquired the data. CH analyzed the data. DK and JEP contributed reagents/materials/analysis tools. CH and JEP wrote the paper. All authors edited and approved the manuscript.

Acknowledgements

We would like to thank Karim Soliman for his guidance in the creation of the Python data analysis pipeline and visualization of the data. We would like to thank Dr. Daniel Zajic for his help performing the lactate accumulation assay.

Funding

Funded by National Science Foundation Grant IOS-2209383 and IOS-2025832.

Data and resource availability

The datasets (DDA and DIA raw data) supporting the conclusions of this article are available in Panorama Public (https://panoramaweb.org/CH0001JP.url) and ProteomeXchange (PXD067707: https://proteomecentral.proteomexchange.org/cgi/GetDataset?ID=PXD067707).

Reviewer login:

Email: panorama+reviewer361@proteinms.net

Password: 3dqk$TMm1AJbo%

727 **References**

728

729 1. Lipton P. Ischemic cell death in brain neurons. Physiological Reviews. 1999;79(4):1431-
730 568.
731 2. Katchanov J, Harms C, Gertz K, Hauck L, Waeber C, Hirt L, et al. Mild cerebral
732 ischemia induces loss of cyclin-dependent kinase inhibitors and activation of cell cycle
733 machinery before delayed neuronal cell death. The Journal of Neuroscience. 2001;21(14):5045-
734 53.
735 3. Andersson BS, Aw TY, Jones DP. Mitochondrial transmembrane potential and pH
736 gradient during anoxia. American Journal of Physiology - Cell Physiology. 1987;252(4):C349-
737 C55.
738 4. Pamenter ME, Gomez CR, Richards JG, Milsom WK. Mitochondrial responses to
739 prolonged anoxia in brain of red-eared slider turtles. Biology Letters. 2016;12(1):20150797. doi:
740 10.1098/rsbl.2015.0797. PubMed PMID: 26763217; PubMed Central PMCID:
741 PMCPMC4785919.
742 5. Galli GLJ, Richards JG. Mitochondria from anoxia-tolerant animals reveals commons
743 strategies to survive without oxygen. Journal of Comparative Physiology B. 2014;184:285-302.
744 doi: 10.1007/s00360-014-0806-3.
745 6. Hammerman C, Kaplan M. Ischemia and reperfusion injury. The ultimate
746 pathophysiologic paradox. Clinics in Perinatology. 1998;25(3):757-77. doi: 10.1016/S0095-
747 5108(18)30110-6. PubMed PMID: 9779346.
748 7. Salas-Vidal E, Méndez-Cruz FJ, Ramírez-Corona A, Reza-Medina B. Oxygen, reactive
749 oxygen species and developmental redox networks: Evo-Devo Evil-Devils? The International
750 Journal of Developmental Biology. 2021;65(4-5-6):345-56. doi: 10.1387/ijdb.200170es.
751 8. Scherz-Shouval R, Elazar Z. ROS, mitochondria and the regulation of autophagy. Trends
752 in Cell Biology. 2007;17(9):422-7.
753 9. Kirino T. Delayed neuronal death in the gerbil hippocampus following ischemia. Brain
754 Research. 1982;239(1):57-69.
755 10. Cao W, Carney J, Duchon A, Floyd R, Chevion M. Oxygen free radical involvement in
756 ischemia and reperfusion injury to brain. Neuroscience Letters. 1988;88(2):233-8.
757 11. Feder ME, Hofmann GE. Heat-shock proteins, molecular chaperones, and the stress
758 response: evolutionary and ecological physiology. Annual Review of Physiology.
759 1999;61(1):243-82. PubMed Central PMCID: PMCHeat Shock Proteins.
760 12. Crowe KM, Newton JC, Kaltenboeck B, Johnson C. Oxidative stress responses of gulf
761 killifish exposed to hydrocarbons from the Deepwater Horizon oil spill: Potential implications
762 for aquatic food resources. Environmental Toxicology and Chemistry. 2014;33(2):370-4.
763 13. Kültz D. Plasticity and stressor specificity of osmotic and heat shock responses of
764 *Gillichthys mirabilis* gill cells. American Journal of Physiology. 1996;271(4):C1181-C93.
765 PubMed Central PMCID: PMCOsmoregulation.
766 14. Carrasco-Malio A, Díaz M, Mella M, Montoya M, Miranda A, Landaeta M, et al. Are the
767 intertidal fish highly resistant to UV-B radiation? A study based on oxidative stress in *Girella*
768 *laevifrons* (Kyphosidae). Ecotoxicology and environmental safety. 2014;100:93-8.
769 15. Baker DW, Matey V, Huynh KT, Wilson JM, Morgan JD, Brauner CJ. Complete
770 intracellular pH protection during extracellular pH depression is associated with hypercarbia

771 tolerance in white sturgeon, *Acipenser transmontanus*. American Journal of Physiology -
772 Regulatory, Integrative and Comparative Physiology. 2009;296(6):R1868-R80. doi:
773 10.1152/ajpregu.90767.2008.
774 16. Storey KB. Reptile freeze tolerance: Metabolism and gene expression. Cryobiology.
775 2006;52(1):1-16.
776 17. Churchill TA, Storey KB. Dehydration tolerance in wood frogs: a new perspective on
777 development of amphibian freeze tolerance. American Journal of Physiology.
778 1993;265(34):R1324-R32. PubMed Central PMCID: PMCDehydration.
779 18. Belkin DA. Anoxia: Tolerance in Reptiles. Science. 1963;139(3554):492-3. doi:
780 10.1126/science.139.3554.492.
781 19. Bickler PE. Cerebral anoxia tolerance in turtles: regulation of intracellular calcium and
782 pH. American Journal of Physiology. 1992;263(6):R1298-R302. PubMed Central PMCID:
783 PMCAnoxia.
784 20. Mojica EA, Fu Y, Kültz D. Salinity-responsive histone PTMs identified in the gills and
785 gonads of Mozambique tilapia (*Oreochromis mossambicus*). BMC Genomics. 2024;25(1):586.
786 Epub 20240611. doi: 10.1186/s12864-024-10471-3. PubMed PMID: 38862901; PubMed Central
787 PMCID: PMCPMC11167857.
788 21. Dyson MH, Thomson S, Mahadevan LC. Heat shock, histone H3 phosphorylation and the
789 cell cycle. Cell Cycle. 2005;4(1):e64-e-8. PubMed Central PMCID: PMCHeat Shock.
790 22. Kim JM, To TK, Ishida J, Morosawa T, Kawashima M, Matsui A, et al. Alterations of
791 lysine modifications on the histone H3 N-tail under drought stress conditions in Arabidopsis
792 thaliana. Plant & Cell Physiology. 2008;49(10):1580-8. Epub 20080908. doi:
793 10.1093/pcp/pcn133. PubMed PMID: 18779215.
794 23. Ma T, Keller JA, Yu X. RNF8-dependent histone ubiquitination during DNA damage
795 response and spermatogenesis. Acta Biochimica et Biophysica Sinica (Shanghai).
796 2011;43(5):339-45. Epub 20110328. doi: 10.1093/abbs/gmr016. PubMed PMID: 21444325;
797 PubMed Central PMCID: PMCPMC3080603.
798 24. Wang Y, Lyu Y, Tu K, Xu Q, Yang Y, Salman S, et al. Histone citrullination by PADI4
799 is required for HIF-dependent transcriptional responses to hypoxia and tumor vascularization.
800 Science Advances. 2021;7(35):eabe3771.
801 25. Wrann S, Kaufmann MR, Wirthner R, Stiehl DP, Wenger RH. HIF mediated and DNA
802 damage independent histone H2AX phosphorylation in chronic hypoxia. Biological Chemistry.
803 2013;394(4):519-28. doi: 10.1515/hsz-2012-0311.
804 26. Batie M, Fasanya T, Kenneth NS, Rocha S. Oxygen-regulated post-translation
805 modifications as master signalling pathway in cells. EMBO reports. 2023;24(12). doi:
806 10.15252/embr.202357849.
807 27. Das T, Kamle A, Kumar A, Chakravarty S. Hypoxia induced sex-difference in zebrafish
808 brain proteome profile reveals the crucial role of H3K9me3 in recovery from acute hypoxia.
809 Frontiers in Genetics. 2021;12:635904. Epub 20220131. doi: 10.3389/fgene.2021.635904.
810 PubMed PMID: 35173759; PubMed Central PMCID: PMCPMC8841817.
811 28. Batie M, Frost J, Frost M, Wilson JW, Schofield P, Rocha S. Hypoxia induces rapid
812 changes to histone methylation and reprograms chromatin. Science. 2019;363(6432):1222-6. doi:
813 10.1126/science.aau5870.
814 29. Mucci S, Isaja L, Rodriguez-Varela MS, Ferriol-Laffouillere SL, Marazita M, Videla-
815 Richardson GA, et al. Acute severe hypoxia induces apoptosis of human pluripotent stem cells
816 by a HIF-1alpha and P53 independent mechanism. Scientific Reports. 2022;12(1):18803. Epub

817 20221105. doi: 10.1038/s41598-022-23650-7. PubMed PMID: 36335243; PubMed Central
818 PMCID: PMCPMC9637190.
819 30. Wijenayake S, Storey KB. Dynamic regulation of histone H3 lysine (K) acetylation and
820 deacetylation during prolonged oxygen deprivation in a champion anaerobe. Molecular and
821 Cellular Biochemistry. 2020;474(1-2):229-41. doi: 10.1007/s11010-020-03848-x.
822 31. Anchordoguy TJ, Hand SC. Reactivation of ubiquitination in *Artemia franciscana*
823 embryos during recovery from anoxia-induced quiescence. Journal of Experimental Biology.
824 1995;198(6):1299-305. PubMed Central PMCID: PMCAnoxia.
825 32. Liu CL, Martone ME, Hu BR. Protein ubiquitination in postsynaptic densities after
826 transient cerebral ischemia. Journal of Cerebral Blood Flow & Metabolism. 2004;24(11):1219-
827 25.
828 33. Podrabsky J, Wilson N. Hypoxia and anoxia tolerance in the annual killifish
829 *Austrofundulus limnaeus*. Integrative and Comparative Biology. 2016;56(4):500-9. doi:
830 10.1093/icb/icw092.
831 34. Hughes C, Mojica EA, Kültz D, Podrabsky JE. Global maintenance of histone post-
832 translational modifications during the transition into anoxia in embryos of the annual killifish
833 *Austrofundulus limnaeus*. Environmental Epigenetics. 2025;in press:1-32.
834 35. Van HT, Santos MA. Histone modifications and the DNA double-strand break response.
835 Cell Cycle. 2018;17(21-22):2399-410. Epub 20181114. doi: 10.1080/15384101.2018.1542899.
836 PubMed PMID: 30394812; PubMed Central PMCID: PMCPMC6342081.
837 36. Weiner A, Hsieh TH, Appleboim A, Chen HV, Rahat A, Amit I, et al. High-resolution
838 chromatin dynamics during a yeast stress response. Molecular Cell. 2015;58(2):371-86. Epub
839 20150319. doi: 10.1016/j.molcel.2015.02.002. PubMed PMID: 25801168; PubMed Central
840 PMCID: PMCPMC4405355.
841 37. Riggs C, Le R, Kültz D, Zajic D, Summers A, Alvarez L, et al. Establishment and
842 characterization of an anoxia-tolerant cell line, PSU-AL-WS40NE, derived from an embryo of
843 the annual killifish *Austrofundulus limnaeus*. Comparative Biochemistry and Physiology - Part
844 B. 2019;232:11-22. doi: 10.1016/j.cbpb.2019.02.008.
845 38. Fordel E, Thijs L, Martinet W, Schrijvers D, Moens L, DeWilde S. Anoxia or oxygen and
846 glucose deprivation in SH-SY5Y cells: A step closer to the unraveling of neuroglobin and
847 cytoglobin functions. Gene. 2007;398:114-22.
848 39. Hsu KF, Wilkins SE, Hopkinson RJ, Sekirnik R, Flashman E, Kawamura A, et al.
849 Hypoxia and hypoxia mimetics differentially modulate histone post-translational modifications.
850 Epigenetics. 2021;16(1):14-27. Epub 20200701. doi: 10.1080/15592294.2020.1786305. PubMed
851 PMID: 32609604; PubMed Central PMCID: PMCPMC7889154.
852 40. Nagagaki Y, Kozakura Y, Mahandaran T, Fumoto Y, Nakato R, Shirahige K, et al.
853 Histone H3.3 chaperone HIRA renders stress-responsive genes poised for prospective lethal
854 stresses in acquired tolerance. Genes to Cells. 2024;29(9):722-34. doi: 10.1111/gtc.13140.
855 41. Stowell C, Wang L, Arbogast B, Lan J-q, Cioffi GA, Burgoyne CF, et al. Retinal
856 proteomic changes under different ischemic conditions-implication of an epigenetic regulatory
857 mechanism. International Journal of Physiology, Pathophysiology and Pharmacology.
858 2010;2(2):148.
859 42. Zager RA, Johnson AC. Renal ischemia-reperfusion injury upregulates histone-
860 modifying enzyme systems and alters histone expression at proinflammatory/profibrotic genes.
861 American Journal of Physiology-Renal Physiology. 2009;296(5):F1032-F41.

862 43. Zhou A, Simon RP, David L. Nascent proteomes of ischemic-injured and ischemic-
863 tolerant neuronal cells. International Journal of Computational Biology and Drug Design.
864 2011;4(1):40. doi: 10.1504/ijcbdd.2011.038656.
865 44. Martire S, Banaszynski LA. The roles of histone variants in fine-tuning chromatin
866 organization and function. Nature Reviews Molecular Cell Biology. 2020;21(9):522-41. doi:
867 10.1038/s41580-020-0262-8.
868 45. Podrabsky JE, Riggs CL, Duerr JM. Anoxia Tolerance During Vertebrate Development -
869 Insights from Studies on the Annual Killifish *Austrofundulus limnaeus*. In: Padilla P, editor.
870 Anoxia. Rijeka, Croatia: InTech; 2012. p. 3-24.
871 46. Talbert PB, Henikoff S. Histone variants at a glance. Journal of Cell Science.
872 2021;134(6):jcs244749. doi: 10.1242/jcs.244749.
873 47. Singh R, Bassett E, Chakravarti A, Parthun MR. Replication-dependent histone isoforms:
874 a new source of complexity in chromatin structure and function. Nucleic Acids Research.
875 2018;46(17):8665-78. doi: 10.1093/nar/gky768. PubMed PMID: 30165676; PubMed Central
876 PMCID: PMCPMC6158624.
877 48. Boidot R, Branders S, Helleputte T, Rubio LI, Dupont P, Feron O. A generic cycling
878 hypoxia-derived prognostic gene signature: application to breast cancer profiling. Oncotarget.
879 2014;5(16):6947-63. doi: 10.18632/oncotarget.2285.
880 49. Shah S, Verma T, Rashid M, Gadewal N, Gupta S. Histone H2A isoforms: Potential
881 implications in epigenome plasticity and diseases in eukaryotes. Journal of Biosciences.
882 2020;45(1). doi: 10.1007/s12038-019-9985-0.
883 50. Meller CL, Meller R, Simons RP, Podrabsky JE. Patterns of ubiquitylation and
884 SUMOylation associated with exposure to anoxia in embryos of the annual killifish
885 *Austrofundulus limnaeus*. Journal of Comparative Physiology B. 2014;184:235-47. doi:
886 10.1007/s00360-013-0791-y.
887 51. Wellmann S, Bettkober M, Zelmer A, Seeger K, Faigle M, Eltzschig HK, et al. Hypoxia
888 upregulates the histone demethylase JMJD1A via HIF-1. Biochemical and Biophysical Research
889 Communications. 2008;372(4):892-7. doi: https://doi.org/10.1016/j.bbrc.2008.05.150.
890 52. Fabrizio P, Garvis S, Palladino F. Histone methylation and memory of environmental
891 stress. Cells. 2019;8(4):339. doi: 10.3390/cells8040339.
892 53. Kim J, Lee H, Yi SJ, Kim K. Gene regulation by histone-modifying enzymes under
893 hypoxic conditions: a focus on histone methylation and acetylation. Experimental & Molecular
894 Medicine. 2022;54(7):878-89. Epub 20220722. doi: 10.1038/s12276-022-00812-1. PubMed
895 PMID: 35869366; PubMed Central PMCID: PMCPMC9355978.
896 54. Brustel J, Muramoto T, Fumimoto K, Ellins J, Pears CJ, Lakin ND. Linking DNA repair
897 and cell cycle progression through serine ADP-ribosylation of histones. Nature Communications.
898 2022;13(1). doi: 10.1038/s41467-021-27867-4.
899 55. Marnett LJ. Oxyradicals and DNA damage. Carcinogenesis. 2000;21(3):361-70. doi:
900 10.1093/carcin/21.3.361.
901 56. Poltronieri P, Miwa M, Masutani M. ADP-ribosylation as post-translational modification
902 of proteins: Use of inhibitors in cancer control. International Journal of Molecular Sciences.
903 2021;22(19):10829. doi: 10.3390/ijms221910829.
904 57. Bartlett E, Bonfiglio JJ, Prokhorova E, Colby T, Zobel F, Ahel I, et al. Interplay of
905 histone marks with serine ADP-ribosylation. Cell Reports. 2018;24(13):3488-502.e5. doi:
906 10.1016/j.celrep.2018.08.092.

58. Mohapatra J, Tashiro K, Beckner RL, Sierra J, Kilgore JA, Williams NS, et al. Serine ADP-ribosylation marks nucleosomes for ALC1-dependent chromatin remodeling. Elife. 2021;10. Epub 20211207. doi: 10.7554/eLife.71502. PubMed PMID: 34874266; PubMed Central PMCID: PMCPMC8683085.
59. Martinez-Zamudio R, Ha HC. Histone ADP-ribosylation facilitates gene transcription by directly remodeling nucleosomes. Molecular and Cellular Biology. 2012;32(13):2490-502. Epub 20120430. doi: 10.1128/MCB.06667-11. PubMed PMID: 22547677; PubMed Central PMCID: PMCPMC3434492.
60. Bhagat TD, Von Ahrens D, Dawlaty M, Zou Y, Baddour J, Achreja A, et al. Lactate-mediated epigenetic reprogramming regulates formation of human pancreatic cancer-associated fibroblasts. eLife. 2019;8:e50663. Epub 20191101. doi: 10.7554/eLife.50663. PubMed PMID: 31663852; PubMed Central PMCID: PMCPMC6874475.
61. Zhang D, Tang Z, Huang H, Zhou G, Cui C, Weng Y, et al. Metabolic regulation of gene expression by histone lactylation. Nature. 2019;574(7779):575-80.
62. Zhang W, Tan X, Lin S, Gou Y, Han C, Zhang C, et al. CPLM 4.0: an updated database with rich annotations for protein lysine modifications. Nucleic Acids Research. 2022;50(D1):D451-D9. doi: 10.1093/nar/gkab849. PubMed PMID: 34581824; PubMed Central PMCID: PMCPMC8728254.
63. Liu X, Wang J, Boyer JA, Gong W, Zhao S, Xie L, et al. Histone H3 proline 16 hydroxylation regulates mammalian gene expression. Nature Genetics. 2022;54(11):1721-35. doi: 10.1038/s41588-022-01212-x.
64. Gantner BN, Palma FR, Kayzuka C, Lacchini R, Foltz DR, Backman V, et al. Histone oxidation as a new mechanism of metabolic control over gene expression. Trends in Genetics. 2024;40:739-46.
65. Unoki M, Masuda A, Dohmae N, Arita K, Yoshimatsu M, Iwai Y, et al. Lysyl 5-hydroxylation, a novel histone modification, by Jumonji domain containing 6 (JMJD6). Journal of Biological Chemistry. 2013;288(9):6053-62. Epub 20130109. doi: 10.1074/jbc.M112.433284. PubMed PMID: 23303181; PubMed Central PMCID: PMCPMC3585044.
66. Serra-Bardenys G, Peiro S. Enzymatic lysine oxidation as a posttranslational modification. FEBS Journal. 2022;289(24):8020-31. Epub 20211002. doi: 10.1111/febs.16205. PubMed PMID: 34535954; PubMed Central PMCID: PMCPMC10078733.
67. Berlett BS, Stadtman ER. Protein oxidation in aging, disease, and oxidative stress. Journal of Biological Chemistry. 1997;272(33):20313-6. doi: 10.1074/jbc.272.33.20313. PubMed PMID: 9252331.
68. Masson N, Ratcliffe PJ. HIF prolyl and asparaginyl hydroxylases in the biological response to intracellular O_2 levels. Journal of Cell Science. 2003;116(15):3041-9.
69. Trenzado C, Hidalgo MC, García-Gallego M, Morales AE, Furné M, Domezain A, et al. Antioxidant enzymes and lipid peroxidation in sturgeon *Acipenser naccarii* and trout *Oncorhynchus mykiss*. A comparative study. Aquaculture. 2006;254(1):758-67.
70. Fontagné S, Lataillade E, Breque J, Kaushik S. Lipid peroxidative stress and antioxidant defence status during ontogeny of rainbow trout (*Oncorhynchus mykiss*). British journal of nutrition. 2008;100(01):102-11.
71. Wagner JT, Knapp MJ, Podrabsky JE. Antioxidant capacity and anoxia tolerance in *Austrofundulus limnaeus* embryos. Journal of Experimental Biology. 2019;222(12):jeb204347. doi: 10.1242/jeb.204347.

952 72. Lagedroste M, Reiners J, Knospe CV, Smits SHJ, Schmitt L. A structural view on the
953 maturation of lanthipeptides. Frontiers in Microbiology. 2020;11. doi:
954 10.3389/fmicb.2020.01183.
955 73. Brennan DF, Barford D. Eliminylation: a post-translational modification catalyzed by
956 phosphothreonine lyases. Trends in Biochemical Sciences. 2009;34(3):108-14. doi:
957 10.1016/j.tibs.2008.11.005.
958 74. Jones LH. Dehydroamino acid chemical biology: an example of functional group
959 interconversion on proteins. RSC Chemical Biology. 2020;1(5):298-304. doi:
960 10.1039/d0cb00174k.
961 75. Lai K-Y, Galan SRG, Zeng Y, Zhou TH, He C, Raj R, et al. LanCLs add glutathione to
962 dehydroamino acids generated at phosphorylated sites in the proteome. Cell. 2021;184(10):2680-
963 95.e26. doi: 10.1016/j.cell.2021.04.001.
964 76. Bogart JW, Bowers AA. Dehydroamino acids: chemical multi-tools for late-stage
965 diversification. Organic & Biomolecular Chemistry. 2019;17(15):3653-69. doi:
966 10.1039/c8ob03155j.
967 77. Johnson AB, Barton MC. Hypoxia-induced and stress-specific changes in chromatin
968 structure and function. Mutation Research/Fundamental and Molecular Mechanisms of
969 Mutagenesis. 2007;618(1-2):149-62. doi: 10.1016/j.mrfmmm.2006.10.007.
970 78. Kratzmeier M, Albig W, Hanecke K, Doenecke D. Rapid dephosphorylation of H1
971 histones after apoptosis induction. Journal of Biological Chemistry. 2000;275(39):30478-86. doi:
972 10.1074/jbc.M003956200. PubMed PMID: 10874037.
973 79. Cheung WL, Ajiro K, Samejima K, Kloc M, Cheung P, Mizzen CA, et al. Apoptotic
974 phosphorylation of histone H2B is mediated by mammalian sterile twenty kinase. Cell.
975 2003;113(4):507-17. doi: 10.1016/s0092-8674(03)00355-6. PubMed PMID: 12757711.
976 80. Fernandez-Capetillo O, Lee A, Nussenzweig M, Nussenzweig A. H2AX: the histone
977 guardian of the genome. DNA Repair. 2004;3(8-9):959-67. doi: 10.1016/j.dnarep.2004.03.024.
978 81. Xiao A, Li H, Shechter D, Ahn SH, Fabrizio LA, Erdjument-Bromage H, et al. WSTF
979 regulates the H2A.X DNA damage response via a novel tyrosine kinase activity. Nature.
980 2009;457(7225):57-62. doi: 10.1038/nature07668.
981 82. Rossetto D, Avvakumov N, Côté J. Histone phosphorylation. Epigenetics.
982 2012;7(10):1098-108. doi: 10.4161/epi.21975.
983 83. Mojica EA, Kültz D. A strategy to characterize the global landscape of histone post-
984 translational modifications within tissues of nonmodel organisms. Journal of Proteome Research.
985 2024;23:2780−94. Epub 20230825. doi: 10.1021/acs.jproteome.3c00246. PubMed PMID:
986 37624673.
987 84. Root L, Campo A, Macniven L, Con P, Cnaani A, Kültz D. A data-independent
988 acquisition (DIA) assay library for quantitation of environmental effects on the kidney proteome
989 of *Oreochromis niloticus*. Molecular Ecology Resources. 2021;21(7):2486-503. doi:
990 10.1111/1755-0998.13445.
991 85. Kong AT, Leprevost FV, Avtonomov DM, Mellacheruvu D, Nesvizhskii AI. MSFragger:
992 ultrafast and comprehensive peptide identification in mass spectrometry-based proteomics.
993 Nature Methods. 2017;14(5):513-20. Epub 20170410. doi: 10.1038/nmeth.4256. PubMed PMID:
994 28394336; PubMed Central PMCID: PMCPMC5409104.
995 86. Benjamini Y, Hochberg Y. Controlling the false discovery rate: A practical and powerful
996 approach to multiple testing. Journal of the Royal Statistical Society Series B. 1995;57:289-300.
997 doi: 10.1111/j.2517-6161.1995.tb02031.x.

998 87. MacLean B, Tomazela DM, Shulman N, Chambers M, Finney GL, Frewen B, et al.
999 Skyline: an open source document editor for creating and analyzing targeted proteomics
1000 experiments. Bioinformatics. 2010;26(7):966-8. Epub 20100209. doi:
1001 10.1093/bioinformatics/btq054. PubMed PMID: 20147306; PubMed Central PMCID:
1002 PMCPMC2844992.
1003 88. Du P, Zhang X, Huang C-C, Jafari N, Kibbe WA, Hou L, et al. Comparison of Beta-
1004 value and M-value methods for quantifying methylation levels by microarray analysis. BMC
1005 Bioinformatics. 2010;11:587. doi: 10.1186/1471-2105-11-587.
1006 89. Chappell K, Graw S, Washam CL, Storey AJ, Bolden C, Peterson EC, et al. PTMViz: a
1007 tool for analyzing and visualizing histone post translational modification data. BMC
1008 Bioinformatics. 2021;22(1):275. doi: 10.1186/s12859-021-04166-9.
1009 90. Wickham H. Elegant Graphics for Data Analysis. New York: Springer-Verlag; 2016.
1010